The Journal of Neuroscience, July 1, 2001, *21*(13):4609–4624

Differential Expression of Genes Encoding Subthreshold-Operating Voltage-Gated K^+ Channels in Brain

M. J. Saganich, E. Machado, and B. Rudy

Department of Physiology and Neuroscience and Department of Biochemistry, New York University School of Medicine, New York, New York 10016

The members of the three subfamilies (eag, erg, and elk) of the ether-a-go-go (EAG) family of potassium channel pore-forming subunits express currents that, like the M-current (I_M), could have considerable influence on the subthreshold properties of neuronal membranes, and hence the control of excitability. A nonradioactive *in situ* hybridization (NR-ISH) study of the distribution of the transcripts encoding the eight known EAG family subunits in rat brain was performed to identify neuronal populations in which the physiological roles of EAG channels could be studied. These distributions were compared with those of the mRNAs encoding the components of the classical M-current (Kcnq2 and Kcnq3). NR-ISH was combined with immunohistochemistry to specific neuronal markers to help identify expressing neurons. The results show that each EAG subunit has a specific pattern of expression in rat brain. EAG and Kcnq transcripts are prominent in several types of excitatory neurons in the cortex and hippocampus; however, only one of these channel components (erg1) was consistently expressed in inhibitory interneurons in these areas. Some neuronal populations express more than one product of the same subfamily, suggesting that the subunits may form heteromeric channels in these neurons. Many neurons expressed multiple EAG family and Kcnq transcripts, such as CA1 pyramidal neurons, which contained Kcnq2, Kcnq3, eag1, erg1, erg3, elk2, and elk3. This indicates that the subthreshold current in many neurons may be complex, containing different components mediated by a number of channels with distinct properties and neuromodulatory responses.

Key words: EAG; ERG; ELK; Kcnq; potassium channels; M-currents; mRNA; nonradioactive in situ *hybridization; immunohistochemistry; GABAergic interneurons; parvalbumin; brain*

Potassium channels that are open at membrane potentials close to the threshold for action potential generation have a major influence on neuronal excitability governing the responsiveness of neurons to incoming inputs. The classical example is the M-current (I_M), first described in sympathetic neurons (Brown and Adams, 1980) and later found in central neurons (Brown, 1988; Yamada et al., 1989). I_M becomes significant above −60 mV and thus may influence the resting potential and the input resistance of the cell. The current opposes depolarizing signals and influences the responsiveness of the cell to synaptic inputs. Moreover, the channels mediating this current (M-channels or M-type K^+ channels) do not inactivate, contributing K^+ current during long depolarizations and producing adaptation in repetitive firing neurons. The inhibition of I_M by neurotransmitters and neuropeptides generates slow depolarizing synaptic potentials and mediates increases in excitability. Another example is subthreshold-activating A-type K^+ channels. These inactivating channels have been shown to regulate the delay between membrane depolarization and action potential generation (delay to first spike) and to modulate firing frequency during repetitive activity (Connor and Stevens, 1971; Rudy, 1988; Baxter and Byrne, 1991; Hille, 1992). They are prominently expressed in dendrites, where they regulate the back-propagation of action potentials from the soma into the dendritic tree and allow cells to filter fast synaptic inputs (Hoffman et al., 1997; Johnston et al., 1999; Schoppa and Westbrook, 1999).

It was shown recently that the classic M-channel in sympathetic neurons is a heteromeric protein containing Kcnq2 and Kcnq3 subunits (Wang et al., 1998). All of the eight known members of the EAG family of K^+ channel pore-forming subunits express homomeric subthreshold- or near threshold-operating K^+ channels, when expressed in heterologous expression systems (see Table 3). Moreover, similar to I_M, some EAG currents do not inactivate and can contribute an M-like steady outward current during long depolarized potentials. Even for EAG family channels that display inactivation, a large component of noninactivating current is present.

The EAG family is subdivided into three subfamilies [eag, erg (eag-related genes), and elk (eag-like K^+ channels)] on the basis of sequence similarities (Warmke and Ganetzky, 1994; Ganetzky et al., 1999). [Because the term EAG is the name of the entire family as well as the name of one of the subfamilies, we have used capital letters (EAG) when referring to the family and lowercase when referring to the subfamily or individual subfamily members.] In the better-studied Kv family of K^+ channel pore-forming subunits, members of the same subfamily (or closely related subfamilies), but not of different subfamilies, can interact to form heteromultimeric channels, often with novel functional properties, resulting in a large increase in the diversity of voltage-gated K^+ channels (McCormack et al., 1990; for review, see Coetzee et al., 1999). Preliminary evidence suggests that members of the same EAG subfamily can also express heteromeric channels in

Received Jan. 9, 2001; revised March 14, 2001; accepted March 22, 2001.

This research was supported by National Science Foundation Grant IBN 0078297 and National Institutes of Health Grants NS30989 and NS35215 to B.R. M.S. is supported by National Research Service Award NS11131, and E.M. is supported by a Minority Supplement to Grant NS35215. We thank Dr. Harriet Baker and Dr. Catherine Priest for ISH protocols and helpful discussions, and D. McKinnon and J. Dixon for the elk1 cDNA.

Correspondence should be addressed to B. Rudy, Department of Physiology and Neuroscience, New York University School of Medicine, 550 First Avenue, New York, NY 10016. E-mail: Rudyb01@med.nyu.edu.

Table 1. NR-ISH probe information

Probe	Accession number	Primers	Position/size		% Identity/gaps[a]	
eag1	Z34264	*Eco*RI restriction fragment from partial eag1 clone from phage screening	2175		w/Eag2	57/6
		*Eco*RI @ pos 2175 and polylinker EcoRI from pBluescript	3087	912 bp		
eag2	AF185637	Forward: CGGAAGGTTTT(CT)(AG)A(N)GA(AG)CA(CT)C	1849		w/Eag1	64/5
		Reverse: CTGCTCGGG(TGA)AT(TGCA)GG(GA)TA(GA)AA	2937	1089 bp		
erg1	Z96106	Forward: GACCTGCA(CT)AAGAT(CT)CA(GT)CGAG [ERGfam]	2491		w/Erg2	47/7
		Reverse: GGGAAACCTGAGAAAGCGAGT	3349	858 bp	w/Erg3	42/7
erg1b	Z96106	Forward: GAGCTGCTTCCTGTGTTTGG	309		w/Erg2	36/18
		Reverse: CTATGATTTCCCGGTCACTG	1084	776 bp	w/Erg3	52/12
erg2	AF016192	Forward: [ERGfam]	2074		w/Erg1	40/7
		Reverse: CCTGTAAGCTACCTCTGAGCA	3137	1063 bp	w/Erg3	38/6
erg3	AF016191	Forward: [ERGfam]	2676		w/Erg1	45/6
		Reverse: GAGACCCAAGATCCCTACAGT	3731	1055 bp	w/Erg2	38/6
elk1	AF061957	Forward: GATCGT(GAC)GATGG(AC)ATTGA(AG)GA [ELKfam]	2490		w/Elk2	36/9
		Reverse: CAGTATAGAGGTGGCTCTGC	3521	1031 bp	w/Elk3	36/8
elk2	AJ007627	Forward: [ELKfam]	2500		w/Elk1	35/9
		Reverse: GACAGAGGACAGTGGAGATG	3523	1023 bp	w/Elk3	44/7
elk3	AJ007628	Forward: [ELKfam]	2572		w/Elk1	36/8
		Reverse: GAATGCTTTGAGCTGCTGGC	3514	942 bp	w/Elk2	45/7
Kcnq2	AF087453	Forward: TCGATGACAGCCCAAGCAAG	2916		w/Kcnq3	46/8
		Reverse: CAACCCACACTACTCTATGC	4221	1305 bp	w/Kcnq4	38/36
					w/Kcnq5	44/4
Kcnq2b	AF087453	Forward: CGCAAGCTGCAGAATTTCCT	1774		w/Kcnq3	64/5
		Reverse: GTAGGTGTCGAAGTGGTCAT	2344	570 bp	w/Kcnq4	73/0
					w/Kcnq5	68/0
Kcnq3	AF091247	Forward: GATGCCATAGAAGAAAGCCC	1326		w/Kcnq2	45/9
		Reverse: CACATGAGTCCAGAAGAGTC	2247	921 bp	w/Kcnq4	42/14
					w/Kcnq5	42/12

[a]Identity to closest relatives. Full-length genes were first aligned using Clustal W. Matching residues and residues aligning with gaps within the probe region were then counted and divided by probe length for percentage.

heterologous expression systems (Wimmers et al., 2001). Many neurons in the CNS coexpress multiple Kv subunits, and heteromeric Kv channels have been shown to exist in native cells (Sheng et al., 1993; Wang et al., 1993; Chow et al., 1999; Hernández-Pineda et al., 1999). Similarly, heteromeric EAG K^+ channels may exist in neurons coexpressing more than one member of the same subfamily.

Moreover, in neurons containing EAG family subunits in addition to Kcnq2–Kcnq3 proteins, the M-like current might be a complex combination of several components mediated by different channels. To begin to understand the modulation of the excitability of different neuronal populations and to facilitate manipulation of these properties, it is necessary to know the distribution of different EAG and Kcnq2 products in CNS neurons. This knowledge is also necessary to select neuronal populations in which the properties and functional roles of native EAG channels might be studied. In this paper, we report a high-resolution mapping of the patterns of expression of mRNA transcripts for the eight known members of the EAG family in the CNS and compare these distributions with those of Kcnq2 and Kcnq3 transcripts.

MATERIALS AND METHODS

RNA probe design and labeling. Antisense RNA probes were prepared for eag1, eag2, erg1, erg2, erg3, elk1, elk2, elk3, Kcnq2, and Kcnq3 potassium channel subunits. The cloning of cDNAs encoding eag2, erg2, erg3, elk2, elk3, Kcnq2, and Kcnq3 subunit fragments was obtained by PCR from single-stranded rat cortex cDNA. The cloning of erg1 was obtained by PCR from rat cerebellum cDNA. Several attempts to amplify elk1 from cortical, cerebellar, or total brain cDNA were unsuccessful. Instead, the elk1 probe was obtained by PCR using the full-length elk1 cDNA clone as the template (gift from D. McKinnon and J. Dixon, State University of New York, Stony Brook). The primers used in all PCRs are listed in Table 2. The thermocycler protocol for all PCRs was as follows: 94°C, 1 min; 55°C, 1 min; 72°C, 1 min; for 35 cycles. Single-stranded cDNA was prepared from random-primed total RNA using Maloney murine leukemia virus-reverse transcriptase (Life Technologies, Gaithersburg, MD) as described previously (Saganich et al., 1999). The eag1 probe was made from a partial eag1 clone obtained from screening a rat brain cDNA library. The details of each probe are listed in Table 1.

Each PCR amplification product was cloned into vectors containing the T7 and/or Sp6 promoters for RNA polymerase, linearized with the appropriate restriction enzyme, and template for *in vitro* transcription prepared by treatment with Proteinase K (10 μg/ml), followed by two phenol/chloroform extractions and ethanol precipitation. Antisense digoxigenin (DIG)-labeled RNA probes (or control sense probes) were made following the manufacturer's protocol by *in vitro* transcription in the presence of DIG-labeled UTP (Roche, Hertforshire, UK) using ~1 μg of template and the appropriate RNA polymerase. The concentration and integrity of each RNA probe was analyzed by gel electrophoresis, and the level of DIG–UTP incorporation was tested by dot blot by comparison to a known DIG-labeled RNA standard (Roche). For each probe, the transcription reaction resulted in ~10 μg of DIG-labeled RNA, which was diluted with RNase-free H_2O (Sigma, St. Louis, MO) to a concentration of 25 ng/μl, aliquoted, and stored at −80°C. All probes were used at a concentration of 50 ng/ml of hybridization buffer in the *in situ* hybridization (ISH) reaction.

To avoid possible cross-reactivity, each probe was designed to include regions of low nucleotide identity with other related family members or other sequences located in the National Center for Biotechnical Information nucleotide database. The highest level of identity found for any probe was calculated to be 73% (Table 1). To further ensure that probes

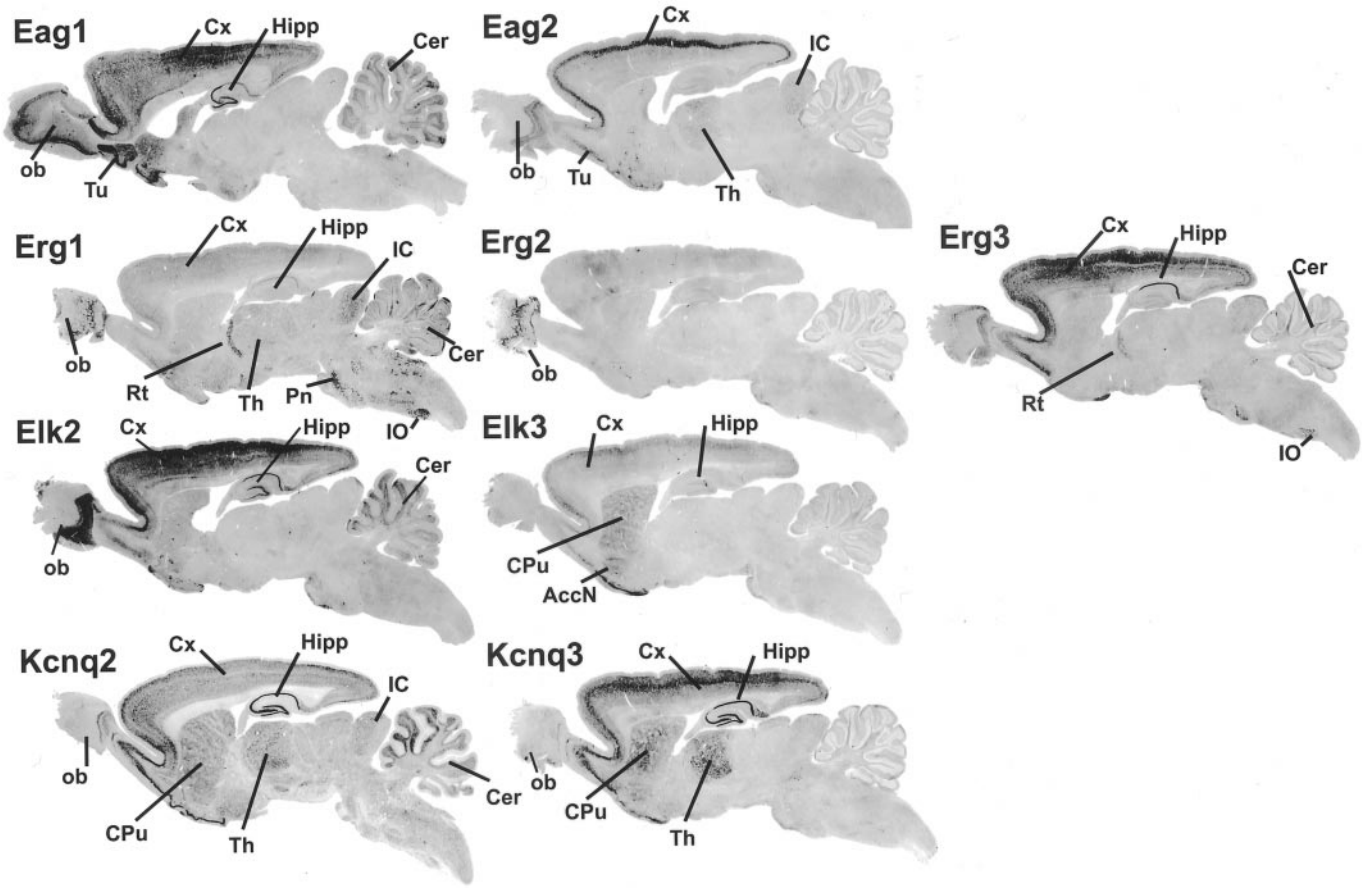

Figure 1. Differential expression of EAG and Kcnq K^+ channels in brain. NR-ISH for EAG family and Kcnq K^+ channel transcripts in rat brain using DIG-labeled RNA antisense probes is shown. DIG-labeled probes were detected using the alkaline phosphatase substrate NBT/BCIP for 14 hr. *AccN*, Accumbens nucleus; *CPu*, caudate/putamen; *Cx*, cerebral cortex; *Cer*, cerebellum; *Hipp*, hippocampus; *IC*, inferior colliculus; *IO*, inferior olive; *ob*, olfactory bulb; *Pn*, pontine nucleus; *Rt*, reticular thalamic nucleus; *Th*, thalamus; *Tu*, olfactory tubercle.

had no cross-reactivity with their closely related subfamily members, we also performed a dot-blot hybridization for each probe against the cDNAs of each EAG family member. As predicted from similarity calculations, each probe proved to be highly specific for its intended EAG subunit when hybridized at the same stringency conditions used in the ISH protocol.

Combined In situ *hybridization–immunohistochemistry.* The nonradioactive (NR)-ISH protocol used was based on a modified radioactive ISH method developed by Dr. Harriet Baker (Burke Medical Research Institute) (Weiser et al., 1994; Saganich et al., 1999). Briefly, 6- to 8-week-old male rats were perfused intracardially with 100 ml of cold saline solution (0.9% NaCl with 0.5% $NaNO_2$ and 1000 U heparin), followed by 300 ml of cold 4% paraformaldehyde solution in 0.1 M phosphate buffer, pH 7.4. The brains were removed carefully, cut in blocks, and post-fixed for 1 hr. After post-fixing, the brains were washed several times in cold, 0.1 M phosphate buffer, pH 7.4, and placed in 30% sucrose overnight. Slices were obtained on a freezing-microtome at 40 μm thickness, and floating sections were prehybridized at 60°C in a solution containing 60% formamide, 3.5× SSC, 5% dextran sulfate, 3.5× Denhardt's solution, 0.5 mg/ml denatured salmon sperm DNA, 0.2 mg/ml t-RNA, and 0.25 mg/ml SDS. After 1 hr of prehybridization, 50 ng/ml of DIG-labeled RNA probe was added, and the hybridization reaction was allowed to proceed for 17 hr.

After hybridization, the sections were washed in decreasing concentrations of SSC (2× to 0.1×) buffer at 65°C followed by a single wash in buffer B1 (150 mM NaCl, 100 mM Tris, pH 7.4) at room temperature. Sections were then treated for 1 hr at room temperature in buffer B1 + 10% normal sheep serum followed by overnight incubation at 4°C with anti-DIG Fab fragments conjugated with alkaline phosphatase (AP) in buffer B1 + 1% normal sheep serum. When co-labeling for neuronal nuclear protein (NeuN), parvalbumin (PV), glutamate decarboxylase (GAD67), and/or calbindin (Cb) was desired, the antibodies were added with the anti-DIG antibodies. Antibodies were used at the following concentrations: anti-DIG Fab, 1:3000 (Roche); NeuN, 1:500 (MAB377; Chemicon, Temecula, CA); PV, 1:500 (Sigma); GAD67, 1:2500 (AB108; Chemicon); Cb, 1:500 (Sigma). Overnight incubation with antibodies was followed by three 15 min washes in buffer B1 followed by 2 hr incubation at room temperature with secondary antibodies (anti-rabbit Cy2 and/or anti-mouse Cy3; Molecular Probes, Eugene, OR) in buffer B1 + 1% normal goat serum + 0.1% BSA + 0.02% cold water fish gelatin. After treatment with secondary antibodies, sections were washed three times for 15 min at room temperature in buffer B1 followed by a single wash in DIG detection buffer (100 mM NaCl, 100 mM Tris, 50 mM $MgCl_2$, pH 9.5). DIG detection was performed using the AP substrate nitro blue tetrazolium/5-bromo-4-chloro-3-indolyl phosphate (NBT/BCIP; Roche) for 8–24 hr in DIG detection buffer. The reaction was stopped by rinsing sections four times for 15 min in ddH_2O; then these were mounted in 0.1× SSC, partially dried, and coverslipped in 50% glycerol on glass slides. Images were acquired using an Olympus Provis microscope equipped with a MagniFire digital camera. Fluorescent images were acquired using filter sets for Cy2 and Cy3.

RESULTS

In situ hybridization is an extremely useful technique for determining the expression pattern of genes of interest in the brain. The development of the NR-ISH method has provided a higher level of resolution as compared with traditional techniques that use radiolabeled probes and photographic emulsion. NR-ISH facilitates identification of individual expressing cells by producing an opaque precipitate within the cell body, rather than silver grains that reside in a layer of emulsion above the cell. Because most of the mRNA in neurons is located within the cytoplasm of

Table 2. Distribution of mRNA for EAG and Kcnq K+ channel subunits in rat brain

	eag1	eag2	erg1	erg2	erg3	elk2	elk3	Kcnq2	Kcnq3
Forebrain									
Olfactory bulb									
Granular cell layer	++	+++	++	−	++	++	−	++	−
Mitral cell layer	+++	+++	++	++	++	++	−	+++	+
Periglomerular layer	−	−	++	++	++	−	−	+	+
Piriform cortex	+++	+++	+	−	++	++	++	+++	+++
Anterior olfactory nucleus	+++	++	−	−	+	+	−	+++	++
Olfactory tubercle	+++	+	−	−	++	+	++	+++	+++
Cerebral cortex									
Layer II	+++	+	+	−	+++	++	++	+++	++
Layer III	+++	++	+	−	+++	++	++	+++	+++
Layer IV	+++	+++	+	−	+	+/−	+	+/−	+++
Layer V	++	+f	+	−	++	+	+	+++	++
Layer VI	++	−	+/−	−	+	+	+	++	+
Inhibitory interneurons	−	−	++[a]	−	−	−	−	+f	−
Hippocampus									
Pyramidal cells									
CA1	++	−	++	−	+++	++	+	+++	+++
CA2	+++	−	−	−	−	+/−	−	+++	+
CA3	+++	+/−	−	−	−	+/−	−	+++	+++
DG	++	+/−	−	−	−	++	+	+++	+++
Inhibitory interneurons	−	−	++	−	−	−	−	−	−
Septum	+	+/−	++	−	+/−	−	−	++	+
Basal ganglia									
Caudate/putamen	++	−	Int	−	+/−	+	++	++	+++
Accumbens nucleus	++	−	−	−	−	−	++	++	++
Globus pallidus	−	−	+	−	−	−	−	+/−	+/−
Thalamus									
Medial geniculate nucleus	−	++	++	−	++[b]	−	−	++	+++
Ventral posterior thalamic complex	−	++	++	−	+/−	−	−	++	+++
DLG	−	++	++	−	+/−	−	−	++	+++
Reticular thalamic nucleus	−	−	+++	−	++	−	−	++	+++
Habenula	+	++	++	−	+	−	−	++	−
Mammilary nucleus	+++	−	++	−	−	−	−	+	+
Amygdala	++	++[c]	+	−	+	++	−	++	++
Hypothalamus	++	+	++	−	+/−	−	−	++	++
Midbrain									
Superior colliculus									
SuG	−	+	+	−	++	+	−	+	++
InG	−	++	+	−	++	+	−	+	++
Inferior colliculus	+	+++	+++	−	+	−	−	++	++
Substantia nigra									
Pars reticulata	−	−	+f	−	−	−	−	+f	++
Pars compacta	−	−	++	−	−	−	−	++	+
Nucleus lateral lemniscus	−	+++	+++	−	+++	−	−	+	+
Ventral tegmental nucleus	−	−	+++	−	−	−	−	+++	+
Raphe nucleus	−	+	+++	−	++	−	−	+	++
Central gray	+	+	+	−	+	−	−	+	+
Red nucleus	++	−	+++	−	−	−	−	++	+++
Oculomotor nucleus (3)	++	−	+++	−	−	−	−	++	+
Hindbrain									
Cerebellum									
Granule layer	+++	−	++	−	−	++	−	+++	−
Molecular layer	−	−	−	−	−	−	−	−	−
Purkinje cell layer	−	−	+++	−	++	−	−	+++	−
Deep nuclei	+	−	+++	−	+	−	−	++	+/−

Table 2 continues.

Table 2. Continued

	eag1	eag2	erg1	erg2	erg3	elk2	elk3	Kcnq2	Kcnq3
Pontine nucleus	+	++	+++	−	−	−	−	++	+
Superior olive	++	++	++	−	+	−	−	+	−
Vestibular nucleus	+	+/−	+++	−	−	−	−	+	+
Dorsal cochlear nucleus	−	++	+++	−	−	−	−	++	++
Ventral cochlear nucleus	−	++	+++	−	−	−	−	+/−	+
Facial nucleus (7)	++	+	+++	−	−	−	−	++	++
Spinal trigeminal nucleus (5)	−	+	+++	−	+	−	−	++	+
Gracile nucleus	−	−	+++	−	++	−	−	+	+
Cuneate nucleus	+	+	+++	−	++	−	−	++	+
Dorsal motor nucleus, vagus (10)	−	−	+	−	++	−	−	−	−
Gigantocellular reticular nucleus	+/−	+/−	+++	−	+/−	−	−	+	+
Hypoglossal nucleus (12)	+	−	++	−	−	−	−	++	+
Lateral reticular nucleus	−	+	+++	−	++	−	−	++	+
Inferior olive	−	−	+++	−	++	−	−	++	++

The data for this table (except for Kcnq2) were generated from NR-ISH of serial coronal sections from the same rat brain in which all genes were processed in parallel in the same experiment under identical conditions. Relative levels of expression were first determined for each individual gene and then normalized between the different genes. +++, Very high; ++, moderate to high; +, low, +/−, just detectable; −, not detectable; f, few neurons; Int, in PV+ interneurons.

[a]Mainly in cingulate cortex.

[b]In amygdala projection nucleus of medial geniculate only.

[c]Eag2 was particularly strong in the intercalated nucleus.

the cell body, the signal produced by NR-ISH usually has a ring or "donut" shape encircling the nucleus. Sometimes the shape of the cell body can be determined from the outline, as observed frequently with relatively abundant transcripts in large layer V pyramidal cells in the cortex, but often the shape of the cell is difficult to obtain.

The regional distribution of EAG and Kcnq K^+ channel transcripts was determined using NR-ISH using DIG-labeled RNA probes. To achieve a higher level of understanding of the distribution of these channel transcripts within heterogenous populations of neurons (such as what is found in the cerebral cortex), this technique was combined with immunohistochemistry using antibodies against NeuN, a marker for all neurons (except, according to the manufacturer, Purkinje, mitral, and photoreceptor cells), and markers for inhibitory neurons: GAD, PV, and Cb (Kawaguchi and Kubota, 1997).

Differential expression of EAG and Kcnq K^+ channel transcripts in rat brain

Each EAG family transcript shows a distinct pattern of expression in rat brain, although some genes have a wider expression pattern than others, as illustrated in representative sagittal images in Figure 1.

The overall pattern of eag1 and eag2 transcripts was similar to previously reported results using lower-resolution methods (Saganich et al., 1999; Ludwig et al., 2000). Eag1 expression was most prominent in the cerebral cortex, hippocampus, cerebellum, and olfactory bulb (Fig. 1, Table 2). Several nuclei of the amygdala and the caudate/putamen also showed prominent expression. Eag1 transcripts were not detected in the thalamus, and only low levels were detected in the brainstem. Unlike eag1, overall expression of eag2 was much more restricted (Fig. 1, Table 2). Eag2 was very abundant in the cerebral cortex and olfactory bulb. Lower levels were also detected in the thalamus, inferior colliculus, intercalated nucleus of the amygdala, and a few brainstem nuclei. Unlike eag1, little or no expression was detected in the hippocampus and cerebellum.

Erg1 is mostly known for its role in the heart, where erg1 subunits combine with accessory mink proteins to form the channels responsible for the IKr current (Trudeau et al., 1995; Sanguinetti et al., 1995; Abbott et al., 1999). Mutations of this gene in humans cause a form of arrhythmia known as long-QT syndrome (Sanguinetti et al., 1995). Erg2 and erg3 were cloned by homology to erg1 from cDNA derived from superior cervical ganglia. Highly sensitive RNase protection assays suggested that erg1 and erg3, but not erg2, were also expressed in brain (Shi et al., 1997).

In our NR-ISH studies, the three members of the Erg subfamily showed different expression levels and patterns in rat brain (Fig. 1). Overall, erg1 levels were low, except for select brain regions. Low levels of erg1 expression seemed to be found in almost every region of the brain; however, in the reticular thalamus, olfactory bulb, and several brain stem nuclei, erg1 expression was more abundant. The widespread low-level expression of erg1 was also found using a separate, non-overlapping probe (erg1b) (Table 1) from a different region of the gene and is therefore believed not to be the result of nonspecific background. Erg3 expression was more abundant but also showed a highly specific pattern of expression, being very prominent in the cerebral cortex, olfactory bulb, and hippocampus. Similar to erg1, erg3 was also found in a few brainstem structures (Table 2). Among EAG family members, erg1 and erg3 were the most prominently expressed transcripts in the brainstem. Interestingly, although RNase protection assays suggested that erg2 is not found in brain (Shi et al., 1997), significant levels of erg2 mRNA were detected in the olfactory bulb. It is possible that the olfactory bulb was not included in the tissue isolated to prepare brain mRNA for the RNase protection assays. Low levels of erg2 (undetectable above normal background using NR-ISH), however, may also be found in the neocortex because the probe was derived from an RT-PCR using total RNA from rat brain cortex (see Materials and Methods). Erg2 had by far the most restricted pattern of expression observed in this study.

The mRNAs of the Elk subfamily also had specific patterns of expression (Fig. 1). Of the three members, elk2 was the most abundant with an overall pattern similar to eag1, with expression

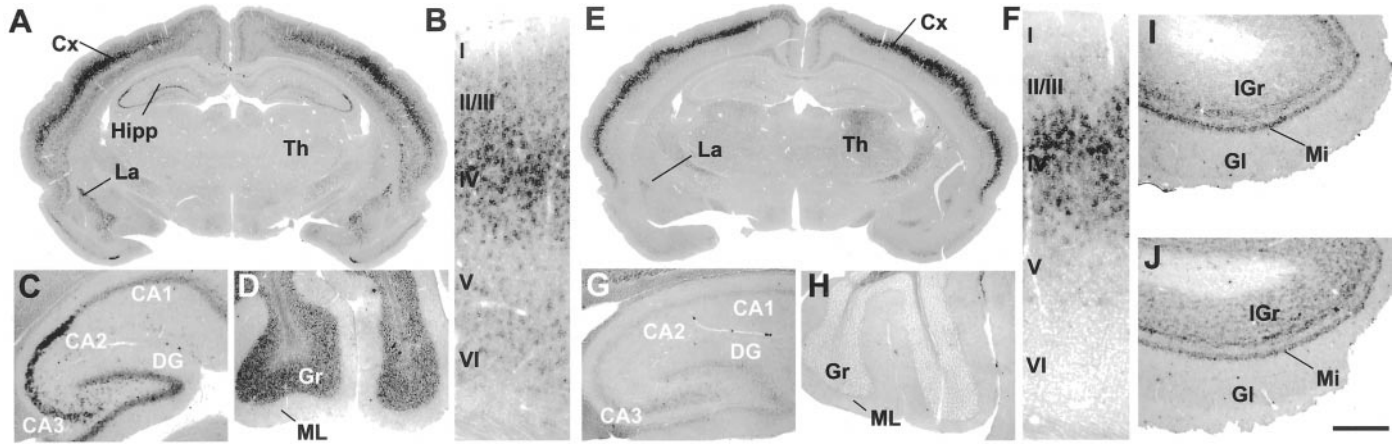

Figure 2. Eag1 and eag2 transcripts have overlapping expression in the cerebral cortex, olfactory bulb, and amygdala. *A–D*, ISH with DIG-labeled eag1 antisense probe. *A*, Eag1 expression in coronal section at the level of the hippocampus showing strong labeling in the cerebral cortex (*Cx*), hippocampus (*Hipp*), and lateral nuclei of the amygdala (*La*). *B*, High magnification of *A* showing eag1 expression in the cerebral cortex with specific lamina identified. Note labeling in layers II–VI, with particular high expression levels in layer IV. *C*, Eag1 expression in the hippocampus showing strongest signals in the CA2 and CA3 fields and in the dentate gyrus (*DG*). *D*, Eag1 staining of the granule cell layer (*Gr*) of the cerebellum. *E–H*, ISH using eag2 DIG-labeled antisense probe. *E*, Eag2 expression in serial section of the same brain as *A*. Note strong expression in cerebral cortex (*Cx*) and much weaker signals in the thalamus (*Th*) and lateral amygdala (*La*). *F*, High magnification of the cortex shows eag2 expression in layer IV. Unlike eag1, little or no eag2 expression was found in the hippocampus (*G*) or the cerebellar cortex (*H*). *I–J*, Overlapping expression of eag1 (*I*) and eag2 (*J*) transcripts was also found in the internal granule layer (*IGr*) and the mitral cell layer (*Mi*) of the olfactory bulb. Scale bar (shown in *J*): *A*, *E*, 1500 μm; *B*, *F*, 150 μm; *I*, *J*, 500 μm; *C*, *D*, *G*, *H*, 600 μm. *ML*, Molecular layer of the cerebellum; *Gl*, periglomerular layer of the olfactory bulb.

in the cerebellum, cerebral cortex, olfactory bulb, and hippocampus. Elk3 expression was relatively weak but very restricted. Like elk2, elk3 was also located in the cerebral cortex; however, it was most prominent in the caudate/putamen and the accumbens nuclei. In this study, the only other transcripts that had similar staining patterns in the caudate were eag1, Kcnq2, and Kcnq3. Our regional results for elk2 and elk3 were in good agreement with Northern blot data of the human Elk homologs bec1 and bec2 (Miyake et al., 1999). Finally, no elk1 expression was found in rat brain. Furthermore, several attempts to amplify elk1 by RT-PCR, using the same RNA that yielded all other members of the EAG and Kcnq families, was unsuccessful (see Materials and Methods), although the primers and PCR conditions tested allowed robust amplification of elk1 when using elk1 cDNA as template. The finding of undetectable levels of elk1 by our ISH methods in rat brain is in agreement with previously reported RNase protection assays that ranked elk1 expression as "just detectable" (Shi et al., 1998). However, a partial elk1 sequence was isolated from rat cortex cDNA by RT-PCR (Engeland et al., 1998). Therefore, the overall expression of elk1 in brain must be very low and requires highly sensitive methods, such as PCR, for detection.

Figure 1 also shows the results of NR-ISH for Kcnq2 and Kcnq3 (see also Table 2). The localization of Kcnq2 in rat brain was extensive, being found to some degree or another in most brain areas (Schroeder et al., 1998; Tinel et al., 1998). The widespread distribution of kcnq2 was also confirmed using a second probe (kcnq2b) from a different region of the gene (Table 1). The highest levels of expression were detected in the hippocampus, cerebral cortex, olfactory bulb, caudate, and cerebellum. Interestingly, Kcnq3 expression was more restricted than Kcnq2 (see implications in Discussion). The highest levels of this transcript were found in the cerebral cortex, thalamus, hippocampus, and caudate/putamen. Several nuclei of the amygdala and the hypothalamus also demonstrated Kcnq3 expression. In the brainstem, expression of both Kcnq2 and Kcnq3 was moderate to weak, but the patterns of both were highly overlapping (see Fig. 12, Table 2).

Analysis at higher magnification, as well as dual staining with antibodies to the neuronal marker NeuN and to markers of GABAergic neurons, allowed the scoring of the expression levels of EAG and Kcnq transcripts in many neuronal populations throughout the brain (Table 2). This analysis and the data shown in Figure 1 show clearly that there is overlap between members of the same subfamily in several neuronal populations. Furthermore, many neurons in the brain express multiple EAG and Kcnq transcripts. Some examples of the data used to generate Table 2 are shown below. We illustrate examples that emphasize the absence or presence of overlap.

Overlapping expression of EAG and Kcnq transcripts

The eag subfamily

Eag1 and eag2 transcripts have overlapping expression in the cerebral cortex and the olfactory bulb (Fig. 2). Serial coronal sections hybridized with eag1 or eag2 antisense probes were used to characterize the expression of both transcripts in the cortex (Fig. 2*A*,*E*). Eag1 expression in the cortex was strongest in layers IV and VI (Fig. 2*A*,*B*). Eag2 expression, however, was much more restricted to the lower layer III and layer IV (Fig. 2*E*,*F*). Products of both genes were seen in the majority of neurons in layer IV (Fig. 3). Co-staining with antibodies to GAD showed that neither eag1 nor eag2 is expressed in inhibitory neurons within layer IV or any other layer in the cortex (Fig. 3). Together the data suggest that eag1 and eag2 are most likely found within the same excitatory neurons in layer IV.

Strong expression of eag1 was also found in the hippocampus and the cerebellum (Fig. 2*A*,*C*,*D*). Higher magnification of the hippocampus showed eag1 to be strongest within the pyramidal layers of the CA2 and CA3 subfields and the granule cell layer of the dentate gyrus (Fig. 2*C*). In contrast, little or no expression of eag2 was found within the hippocampus (Fig. 2*G*). In the cerebellum, eag1 was very strong and restricted to the granule cell

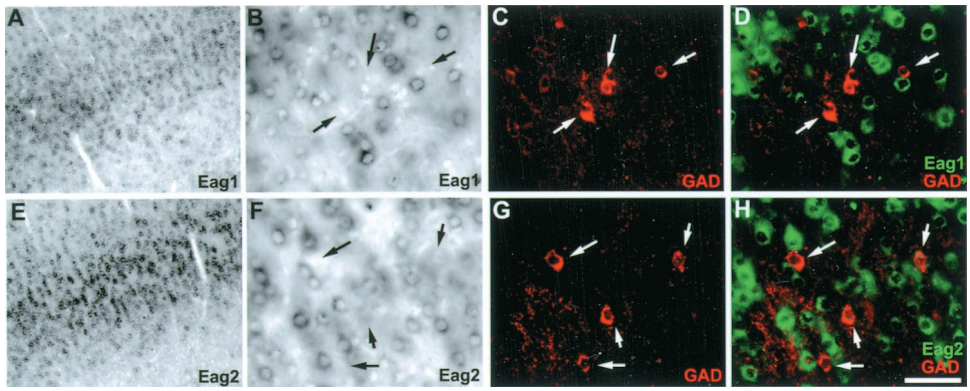

Figure 3. Eag1 and eag2 transcripts are not found in inhibitory cells of the cortex. *A–D*, Dual detection of eag1 and GAD in cortical layer IV. *A*, Low-magnification bright-field image of eag1 expression in cortical layer IV. *B*, High-magnification bright-field image of *A* showing eag1 expression in many small non-pyramidal neurons. *C*, Immunofluorescent detection of GAD immunoreactive interneurons. *D*, Overlay of *B* and *C* with eag1 expression pseudocolored *green*. Note GAD+ neurons are not labeled for eag1 (*arrows*). *E–H*, Same as *A–D*, but for eag2. Note eag2 transcripts do not colocalize with GAD+ immunoreactive neurons (*arrows*). Scale bar (shown in *H*): *B–D*, *F–H*, 50 μm; *A*, *E*, 200 μm.

layer (Fig. 2*D*). In contrast, little eag2 expression was found within the cerebellum (Fig. 2*H*).

Expression of eag1 and eag2 was also found to colocalize within the olfactory bulb (Fig. 2*I*,*J*). In the case of both genes, expression was found in the mitral cell layer and the granule cell layers of the olfactory bulb. In contrast, neither gene was found within cells of the periglomerular region of the bulb.

One of the most striking features of eag2 expression in brain is its specific laminar expression in the neocortex (Figs. 1, 2) (Saganich et al., 1999). Using radioactive probes, we were unable to ascertain which neurons were expressing the gene, both because of the lack of delineation of neuronal morphology with radioactive ISH on Nissl counter-stained sections, as well as the fact that given the cell density in layer IV it was very difficult to assign emulsion grains to underlying cells. NR-ISH showed that the laminar distribution of eag2 transcripts varied with cortical region, being most abundant in the somatosensory cortex as compared with other cortical areas (Fig. 4*A*). In tangential sections through the rat somatosensory barrel cortex, a barrel pattern with hollow centers is observed after NR-ISH for eag2 (Fig. 4*B*), indicating that eag2 transcripts are concentrated in spiny stellate cells (Egger and Sackmann, 2001). In coronal sections, it is also clear that the strongest hybridization signals are seen in the barrel sides and barrel margins with layer III and layer V (Fig. 4*C–E*). Many of the neurons prominently expressing eag2, in the barrel margin with layer III, have clear pyramidal morphology (Fig. 4*I–K*), whereas those inside layer IV are small, non-pyramidal or have a star-shaped appearance (Fig. 4*F–H*).

The Erg subfamily

As mentioned above, the three members of the Erg family have very different distributions. Overlap of two or more of the *Erg* genes does occur, however, in several areas (Figs. 5-7). For example, expression of both erg1 and erg3 was seen in the reticular thalamus (Fig. 5*A*,*B*). Given that the reticular thalamus is composed mainly of a single population of GABAergic neurons (Jones 1985), and that most neurons in this nucleus express erg1 and erg3 (data not shown), each reticular thalamus neuron most likely expresses both transcripts. This was confirmed after co-labeling with antibodies to GABA and PV (data not shown). The reticular thalamus is in fact one of the areas in which erg1 is most abundant. Erg3 expression is much weaker than erg1 in the reticular thalamus as well as in dorsal thalamic nuclei (Fig. 5*B*). Erg1 is expressed throughout the dorsal thalamus, but at lower levels than in the reticular thalamus (Fig. 5*A*, Table 2).

Both erg1 and erg3 transcripts were also expressed in the cerebral cortex (Figs. 5*A–D*, 7). Erg1 expression in the cortex was much weaker than erg3 and was found throughout all layers of the cortex (Fig. 5*C*). In contrast, erg3 expression in the cortex was very strong and produced a bilaminar pattern easily observed at low magnification (Fig. 5*B*). This pattern was the result of strong staining of neurons within cortical layer II/III and layer V (Fig. 5*D*). Weaker staining was also apparent in layers IV and VI. High-magnification images of the erg3 *in situ* experiments and co-labeling with NeuN antibodies (as performed for eag2 above) confirmed that erg3 transcripts in layers III and V were found mostly within neurons with pyramidal morphology (data not shown). Unfortunately, the weak expression of erg1 transcripts in the cortex made more detailed characterization of this gene product difficult (with the exception of the cingulate and retrosplenial cortices; see below). However, it was clear, on the basis of co-labeling with NeuN antibodies, that erg1, like erg3 transcripts, was located within most large layer V pyramidal neurons (Fig. 5*C*).

Both erg1 and erg3 are found within the cerebellum as well (Fig. 5*E*,*F*). Erg1 is located within the granule cell layer and in Purkinje cells. Because of the small amount of cytoplasm found within cerebellar granule neurons, and background from fibers, it is easier to appreciate the granule layer staining at lower magnifications (Fig. 5*E*, *top panel*). Higher magnifications reveal clear labeling of the large Purkinje cells at the border of the granule cell layer (Fig. 5*E*, *bottom panel*). Unlike erg1, erg3 expression was extremely weak in the granule cell layer (Fig. 5*F*, *top panel*). However, as observed for erg1, this transcript was expressed in Purkinje neurons (Fig. 5*F*, *bottom panel*).

All three Erg transcripts were expressed within the olfactory bulb (Fig. 5*G*). Erg1 and erg3 had similar patterns, being located within the majority of neurons of the mitral cell and granule cell layers and in scattered cells within the periglomerular area (Fig. 5*G*, *top* and *bottom panels*). Erg2 expression, which was not found anywhere else in the brain, had an even more restricted pattern in the bulb as compared with its relatives erg1 and erg3. Erg2 was found only in the periglomerular and mitral cell layers, with no

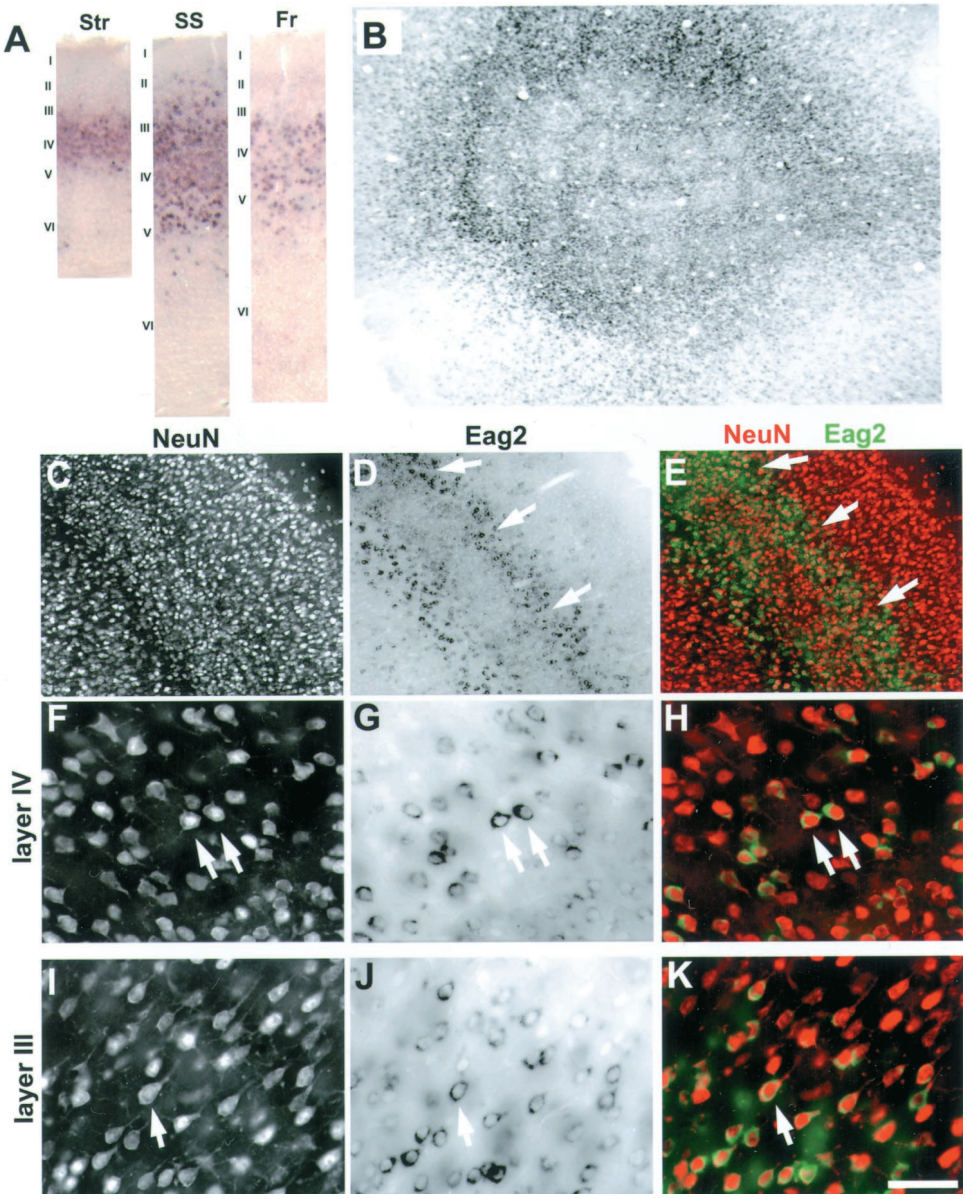

Figure 4. Characterization of eag2 expression in the cerebral cortex. *A*, Changes in eag2 expression with cortical region. Eag2-expressing neurons are more abundant in somatosensory cortex (*SS*) as compared with the striate (*Str*) and frontal (*Fr*) cortical regions. *B*, ISH for eag2 in tangential sections through rat somatosensory barrel cortex reveals a whisker barrel pattern with hollow centers. *C–E*, Combined ISH for eag2 and immunofluorescent detection of NeuN in a coronal section through rat somatosensory barrel cortex. *C*, Fluorescent detection of all neurons using NeuN antibodies. *D*, Same section in bright field showing labeling for eag2 by ISH. Note that eag2 staining demarcated cortical layer IV with strong labeling of neurons lining the barrel sides (*arrows*), as well as neurons on the margins between layer IV and neighboring layers. *E*, Overlay of *C* and *D* with eag2 pseudocolored *green*, and NeuN *red*. *F–K*, High-magnification images of *C* identifying eag2-positive neurons along barrel sides in cortical layers IV (*F–H*) and in deep cortical layer III (*I–K*). Note that eag2-positive neurons in layer IV are small and non-pyramidal and have a star-shaped appearance (*F–H*, *arrows*). In contrast, eag2-positive cells in deep layer III are clearly pyramidal in shape with identifiable apical dendrites that are orientated toward the pia surface (*I–K*, *arrow*). Scale bar (shown in *K*): *A*, 400 μm; *B*, 575 μm; *C–E*, 500 μm; *F–K*, 50 μm.

labeling in the granule cell layer (Fig. 5*G*, *middle*). The staining pattern of erg2 was similar to erg1 and erg3 in the periglomerular region but was different in the mitral cell layer, being found within slightly larger and more scattered cells. Interestingly, high-power images of erg1 within the periglomerular layer revealed that this transcript was found in a small number of neurons, with larger soma size, that did not co-label with PV or Cb (Fig. 8*E–H*). This suggests that erg1 transcripts within the glomerular region of the olfactory bulb are probably expressed in the external tufted cells and not the PV and Cb containing periglomerular or superficial short axon cells (Crespo et al., 1997).

Erg1 and erg3 expression patterns were quite different in the hippocampus but did show some areas of overlap (Fig. 6). Erg1 expression was relatively weak and appeared to be concentrated in the pyramidal cells of the CA1 field and in scattered cells located throughout the hippocampus (Fig. 6*A–G*). Many of these scattered cells located outside or near the pyramidal cell layers were PV positive (Fig. 6*B–G*) and most likely correspond to the inhibitory basket cells (Freund and Buzsaki, 1996). Erg3 was also found within CA1 pyramidal cells, but at much higher levels (Fig. 6*H–N*). Unlike erg1, erg3 expression was restricted to the pyramidal cell layer and was not found in surrounding PV-positive cells (Fig. 6*I–N*).

The expression of erg1 in PV-containing inhibitory neurons in the brain was not restricted to the hippocampus. As mentioned above, erg1, as well as erg3, was located within the reticular thalamus (Figs. 1, 5), in which all neurons are inhibitory PV-expressing neurons (Jones, 1985). In the cerebral cortex, erg1 was also found to be expressed in a population of PV-containing interneurons located within the cingulate and retrosplenial cortices (Fig. 7*A*). Within these areas, the majority, and the strongest erg1-labeled neurons, were PV positive (Fig. 7*B–D*). Interestingly, outside these two cortical areas, it was increasingly difficult to find strongly labeled cells and to show coexpression with PV in the cortex (data not shown). In contrast, erg3 did not co-label with PV-containing interneurons in the cortex (Fig. 7*E–H*). Finally, erg1 was also found to be located within PV-positive cells in the caudate (Fig. 8*A–D*). These neurons, which correspond to locally projecting aspiny interneurons (Kita et al., 1990; Hontanilla et al., 1998), were labeled strongly for erg1, scattered, and few in num-

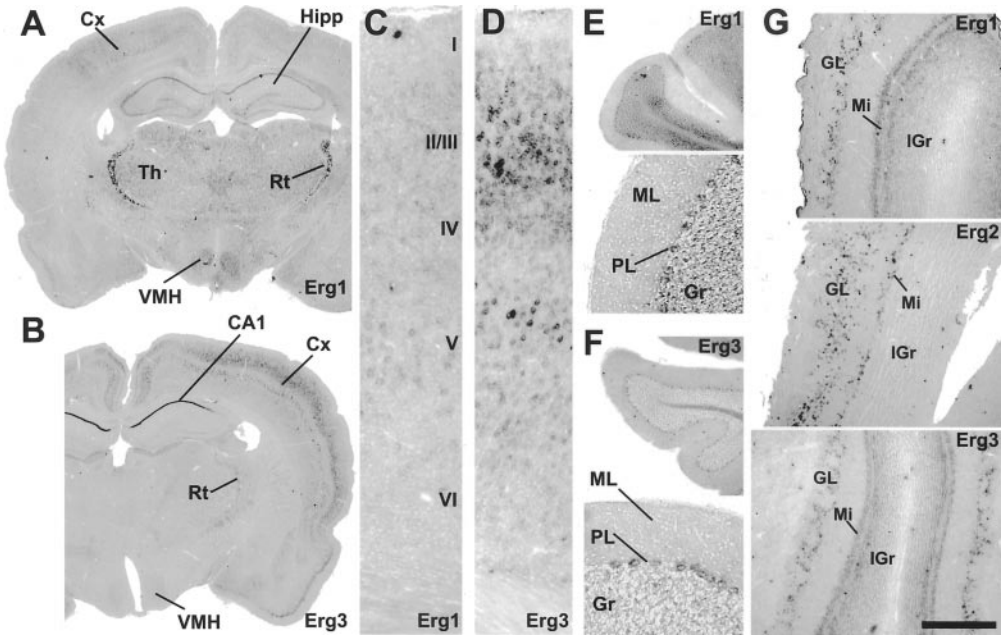

Figure 5. Overlapping expression of Erg mRNA transcripts occurs in the reticular thalamus, cerebellum, hippocampus, and olfactory bulb. *A*, ISH with erg1 antisense probe. Note that erg1 expression was relatively weak with the exception of the reticular thalamic nucleus (*Rt*). Weaker expression was found in the cerebral cortex (*Cx*), hippocampus (*Hipp*), thalamus (*Th*), and ventral medial hypothalamic nuclei (*VMH*). *B*, ISH with erg3 antisense probe. Erg3 expression was strong in the cerebral cortex (*Cx*) and the CA1 subfield of the hippocampus (*CA1*). Weaker erg3 expression was also found in the *Rt* and the *VMH*. *C–D*, Expression of erg1 and erg3 mRNA in cerebral cortex. *C*, High magnification of the cortex in *A* showing weak erg1 expression throughout cortical layers II–V. *D*, High magnification of *B* showing strong erg3-positive neurons in layers II/III and V. *E*, *F*, Expression of erg1 and erg3 transcripts, respectively, in the cerebellar cortex. Note that both transcripts were found in the Purkinje cell layer (*PL*). Comparison at low power revealed that only erg1 was found in the granule cell layer (*E*, *F*, *top panels*). *G*, Colocalization of erg1 (*top*), erg2 (*middle*), and erg3 (*bottom*) in the olfactory bulb. Erg1 and erg3 transcripts were located in neurons of the internal granule layer (*IGr*), mitral cell layer (*Mi*), and periglomerular layer (*GL*). Erg2 transcripts, however, were located only within the mitral cell layer and the periglomerular cell layer. Scale bar (shown in *G*): *A*, *B*, 2000 μm; *C*, *D*, 200 μm; *E*, *F (top)*, 720 μm; *E*, *F (bottom)*, 360 μm; *G*, 500 μm.

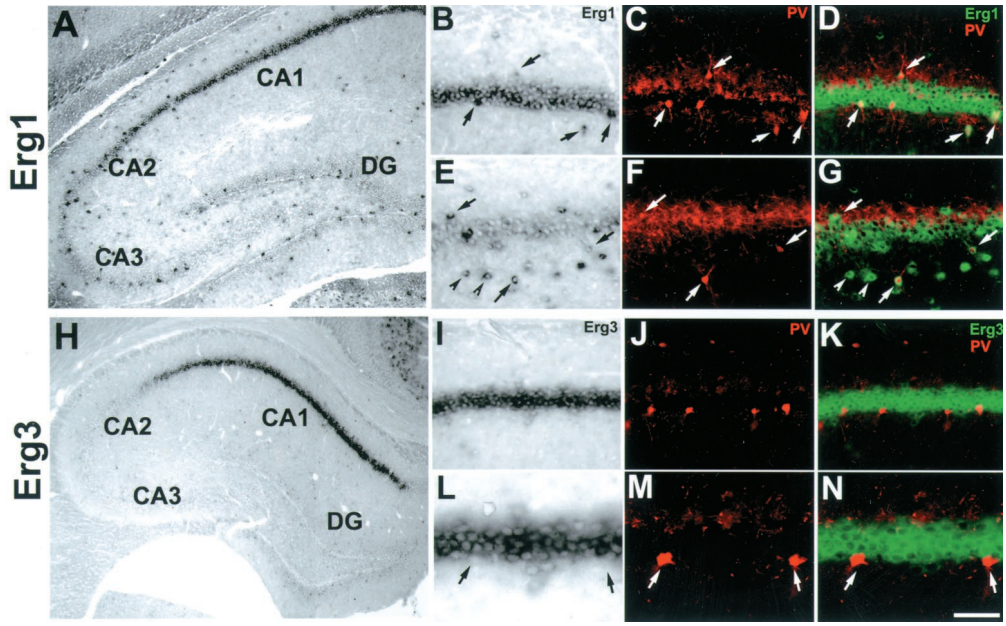

Figure 6. Erg1, but not erg3, is located in PV-containing interneurons throughout the hippocampus, but both are coexpressed in CA1 pyramidal cells. *A–G*, ISH using erg1 antisense probe. *A*, Erg1 expression within the CA1 pyramidal cell layer and scattered cells throughout the hippocampus. *B–D*, Dual labeling for erg1 and PV in the CA1 subfield. *B*, Bright-field image of erg1-positive neurons. *C*, Immunofluorescent detection of PV-reactive interneurons found on the margin of the CA1 pyramidal cell layer. *D*, Overlay of *C* and *D* with erg1 pseudocolored *green*. Note that many of the strongly labeled neurons in *B* are also PV positive (*B–D*, *arrows*). *E–G*, Dual labeling for erg1 and PV in the CA3 hippocampal subfield. *E*, Erg1 expression is found in the pyramidal cell layer and stratum radiatum. *F*, PV immunoreactive interneurons in the CA3 (*arrows*). *G*, Overlay of *E* and *F* with erg1 pseudocolored *green*. Note less erg1 expression in the CA3 pyramidal cell layer as compared with the CA1 (compare *green* cells in *D* and *G*). Similar to the CA1, several PV-positive neurons also expressed erg1 (*E–G*, *arrows*). However, not all erg1-positive neurons located outside the pyramidal cell layer were PV positive (*E*, *G*, *arrowheads*). *H–N*, ISH using erg3 antisense probe. *H*, Erg3 expression was very strong and concentrated on the CA1 hippocampal subfield. *I–N*, Dual labeling of erg3 transcripts and PV-immunoreactive interneurons in the CA1. *I*, Erg3 expression was located within the pyramidal cell layer of the CA1, but not in scattered cells located outside as observed using erg1 probe (compare *B* and *I*). *J*, Immunolocalization of PV+ interneurons located along the CA1 pyramidal cell layer. *K*, Overlay of *I* and *J* with erg3 pseudocolored *green*. *L–M*, High magnification of *I–K*, respectively, showing that erg3 labeling does not colocalize with PV (*arrows*). Scale bar (shown in *N*): *A*, 1000 μm; *B–G*, *I–K*, 100 μm; *H*, 810 μm; *L–N*, 50 μm.

ber (Fig. 8*A*,*B*). In contrast, no erg3 signal was detected in the caudate (Fig. 1, Table 2).

Erg1 was also expressed in several brainstem nuclei (Fig. 1). A more detailed analysis of the pattern of expression in this brain area is presented later to compare the expression of erg1 transcripts with the products of Kcnq genes (see Fig. 12).

The Elk subfamily

Among the two Elk transcripts found in brain, elk2 and elk3, there was little overlap in expression. Elk2 had very strong expression in the granule cell layer of the cerebellum (Fig. 9*A*,*B*). No expression of elk2 was found in the Purkinje cells, which could

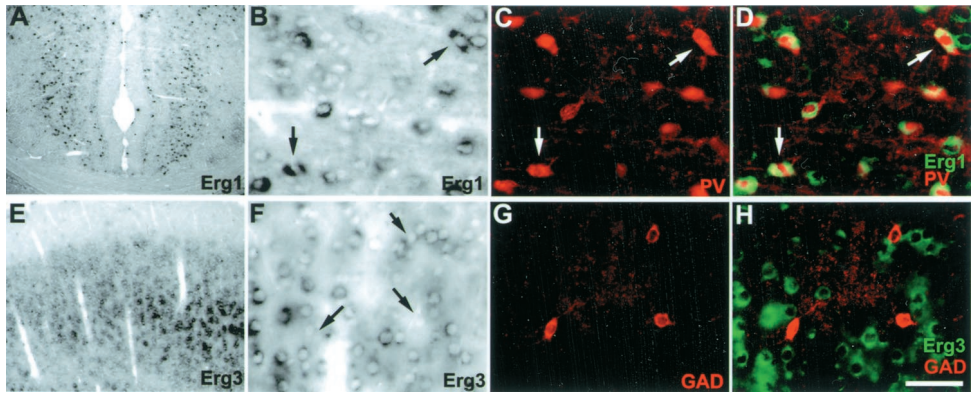

Figure 7. Erg1 is located in a population of parvalbumin-containing interneurons in the cingulate cortex, whereas erg3 is found only in excitatory neurons in the cerebral cortex. *A*, Relatively strong erg1 expression was found within neurons of the cingulate cortex. *B–D*, Identification of a population of erg1-positive interneurons in the cingulate cortex by dual labeling with PV. *B*, High-power bright-field image of erg1-positive neurons from *A*. Note that erg1-positive neurons are scattered and strongly labeled. *C*, Immunofluorescent detection of PV-containing interneurons. *D*, Overlay of *B* and *C* with erg1 signals pseudocolored *green*. Note that nearly all PV-positive neurons are also expressing erg1 transcripts. Characteristic labeling of interneurons by ISH, revealing a bipolar shape, is evident in bright field (*arrows*). *E–H*, Unlike erg1, erg3 expression is not found in inhibitory neurons of the cortex. *E*, Low-power bright-field image showing erg3 expression in cortical layers II/III. *F*, High-magnification bright-field image of erg3-positive cells in cortical layer III. *G*, Immunodetection of GAD-immunoreactive interneurons. *H*, Overlay of *F* and *G* with erg3 signals pseudocolored *green.* Note that GAD-positive cells do not express erg3 (*F*, *arrows* point to unlabeled GAD+ cells). Scale bar (shown in *H*): *A*, *E*, 500 μm; *B–D*, *E–H*, 50 μm.

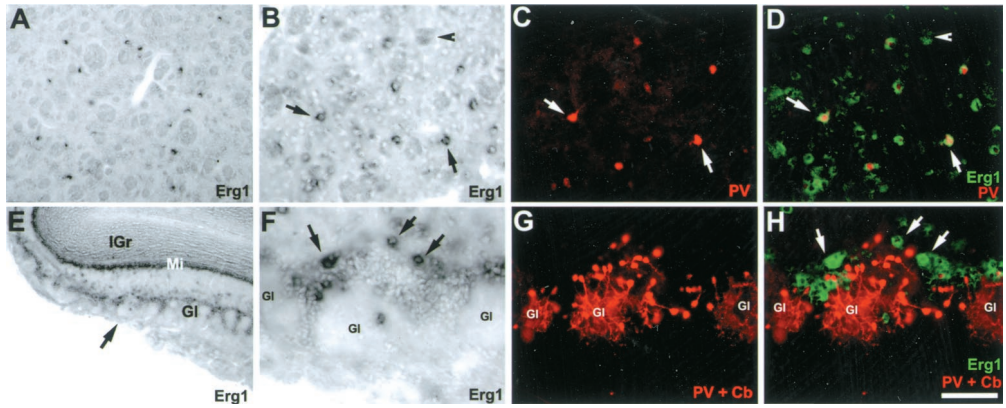

Figure 8. Erg1 transcripts are located in a few scattered PV-positive cells in the caudate/putamen but do not colocalize with PV or Cb in the olfactory bulb. *A–D*, Erg1 transcripts are located in PV-positive interneurons of the caudate/putamen (CPu). *A*, Low-magnification bright-field image of erg1-expressing cells in the CPu. Note that cells are strongly labeled but scattered and few in number. *B*, Higher magnification image of erg1-positive neurons in the CPu. Fiber tracts appear as *light gray* (*arrowhead*). *C*, Immunofluorescent detection of PV-containing neurons. *D*, Overlay of *B* and *C* with erg1 signals pseudocolored *green*. Note that most PV-positive neurons also express erg1 (*B–D*, *arrows*). *E–H*, Erg1-expressing neurons in the periglomerular layer of the olfactory bulb are not immunoreactive for PV or Cb. *E*, Low-magnification bright-field image of erg1 in the olfactory bulb. *F*, High magnification of *E* (*arrow*) showing three glomeruli (*Gl*). Note that erg1 expression is strong and located in large neurons within the periglomerular layer (*arrows*). *G*, Immunofluorescent detection of PV- and Cb-positive periglomerular neurons (PV and Cb monoclonal antibodies were mixed and detected with the same secondary antibody). *H*, Overlay of *F* and *G* with erg1 labeling pseudocolored *green*. Note that none of the large erg1-positive neurons are PV or Cb positive. Scale bar (shown in *H*): *A*, 250 μm; *E*, 500 μm; *B–D*, *F–H*, 100 μm.

be identified by labeling with PV (Fig. 9*B*). In contrast, elk3 was not expressed significantly anywhere in the cerebellum (Fig. 9*C,D*).

Elk2 expression was also strong within the olfactory bulb (Fig. 9*E,F*). At high magnification, it was clear that elk2 was found within both the mitral and granule cell layers (Fig. 9*F*). Elk2 was not found within the cells of the periglomerular layer (Fig. 9*F*). Elk3 expression was not detected in the olfactory bulb (Fig. 1).

In contrast, elk3 expression was relatively strong within the caudate (Fig. 9*G,H*). Higher magnification revealed that most neurons within the caudate were elk3 positive (Fig. 9*H*), suggesting that this transcript is expressed in the principal neurons of this nucleus, the medium spiny neurons (Heimer et al., 1995). This was similar to the pattern observed for eag1 (data not shown) and Kcnq2 and Kcnq3 (Fig. 10) (see below) but unlike the interneuron staining found in the caudate using the erg1 probe (Fig. 8).

Expression of both elk2 and elk3 was observed in the hippocampus (Fig. 9*I–J*). Elk2 signals were much stronger than elk3 in the hippocampus, but they overlapped. Signals for both transcripts were located in the pyramidal cell layer of the CA1 field and the granule cells of the dentate gyrus.

Both elk2 and elk3 were also located in the cerebral cortex (Fig. 9*K–N*). Each gene was found throughout all cortical layers, but both were most abundant within the neurons of the upper lamina (layers II–III).

Kcnq2 and Kcnq3

The overlapping expression of Kcnq2 and Kcnq3 transcripts is of particular interest because it is believed that heteromultimers of these two channel subunits are responsible for the native M-currents that have been recorded within several brain areas, including the cerebral cortex and the hippocampus (Halliwell, 1986; Brown, 1988; McCormick and Williamson, 1989; McCormick, 1992; Wang et al., 1998; Cooper et al., 2000). The lack of overlapping expression of the products of these two genes is also interesting because Kcnq3 homomultimers have been reported to conduct little current in heterologous expression systems (Wang et al., 1998).

The hippocampus was a brain area in which both Kcnq2 and Kcnq3 transcripts were prominent and colocalized in the same neuronal populations (Fig. 10*A,B*). Kcnq2 was located in the pyramidal cell layer of the CA1–CA3 subfields and the granule cells of the dentate gyrus (Fig. 10*A*). Kcnq3 expression in the

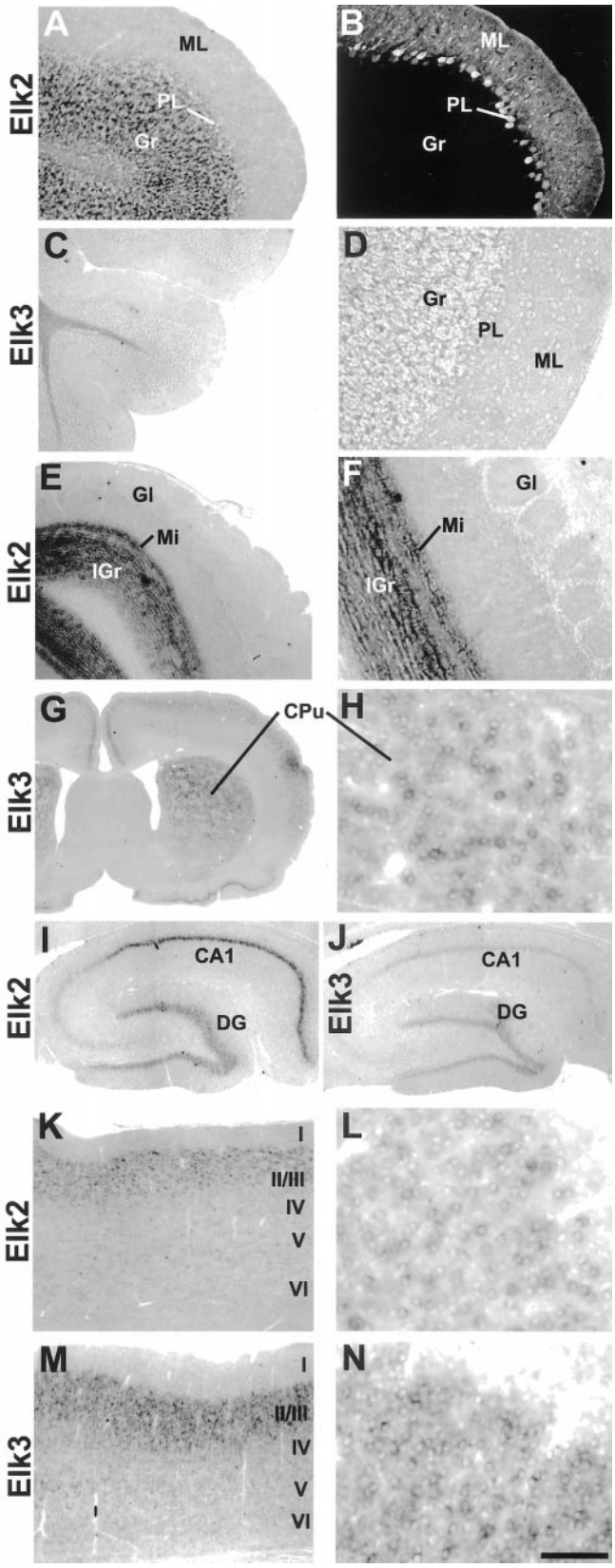

Figure 9. Elk2 and elk3 expression in rat brain have overlapping expression in the cerebral cortex and hippocampus. *A–B*, Dual labeling of elk2 and PV in rat cerebellar cortex. *A*, Bright-field image showing elk2 expression localized to the granule cell layer (*Gr*) of the cerebellum. *B*, Immunofluorescent detection of PV-labeled Purkinje neurons within the Purkinje layer (*PL*) and inhibitory cells within the molecular layer (*ML*). Comparison of *A* and *B* shows that elk2 is not expressed within the Purkinje cell layer as demarcated by PV staining. *C–D*, Low- and high-magnification bright-field images, respectively, showing no elk3 expression within the cerebellar cortex. *E–F*, Low- and high-magnification bright-field images, respectively, showing strong elk2 expression in the olfactory bulb. Elk2 was abundant in the internal granule (*IGr*) and mitral cell (*Mi*) layers but not within the periglomerular area (*Gl*). *G–H*, Elk3 expression in the caudate/putamen (*CPu*). *G*, Low-magnification image showing elk3-positive neurons in the *CPu*. *H*, Higher magnification of *G* showing that most neurons in the *CPu* were elk3 positive (as compared with erg1) (Fig. 8*A*,*B*). *I–J*, Localization of elk2 and elk3 transcripts, respectively, in the hippocampus. Note that both genes were found in the CA1 subfield and the DG, with elk3 expression being weaker than that of elk2. *K–L*, Elk2 expression in the cerebral cortex. *K*, Low-power bright-field image showing weak elk2 expression throughout all the cortical lamina with higher levels in upper layers II/III. *L*, High-power image of *K* showing cortical layer II. Note large number of weakly stained neurons. *M–N*, Elk3 expression in cerebral cortex. *M*, Similar to elk2, elk3 expression was found throughout the cortex with higher levels within upper lamina. *N*, High-power image of *M* showing elk3 in a large proportion of layer II neurons. Scale bar (shown in *N*): *A*, *B*, *D*, *F*, *H*, *L*, *N*, 200 μm; *I*, *J*, 550 μm; *G*, 2000 μm; *C*, *E*, *K*, *M*, 500 μm.

hippocampus was slightly more restricted, being most prominent within the CA1, CA3, and dentate gyrus, but lower in the CA2 subfield (Fig. 10*B*).

Both Kcnq2 and Kcnq3 were expressed in the majority of cells in the caudate (Fig. 10*C*,*G*). Neither Kcnq3 (Fig. 10*D–F*) nor Kcnq2 (data not shown) colocalized with the interneuron marker PV. As for elk3, on the basis of the number and size of the Kcnq2 and 3-labeled neurons, we hypothesize that they correspond to the medium spiny neurons (Heimer et al., 1995). On the other hand, one area in which Kcnq2 and Kcnq3 expression did not overlap was the cerebellar cortex. Kcnq2, but not Kcnq3, was expressed in the cerebellar cortex (Fig. 10*H*). Kcnq2 was prominently expressed in granule and Purkinje cells but not in the interneurons of the molecular layer (Fig. 10*H–K*).

Both Kcnq2 and Kcnq3 were expressed in the cerebral cortex. Kcnq3 was most prominent in layer IV and was present in a large majority of the small abundant cells of this layer, probably colocalizing with eag1 and eag2. In contrast, Kcnq2 signals were negligible in this highly populated cortical lamina (Figs. 1, 11*A*,*H*). Nevertheless both Kcnq2 and Kcnq3 were strongly expressed in most pyramidal cells in layers II–III and V, where they are likely to be coexpressed in the same neurons (Fig. 11*A*,*B*,*E*-,*H*,*I*,*L*). Dual labeling for PV (Fig. 11*I–N*) and GAD (data not shown) showed that Kcnq3 is not expressed in GABAergic interneurons. Interestingly, in some experiments Kcnq2 was seen to colocalize in a few PV-containing cells in layers II–III (Fig. 11*B–D*). Co-labeling of Kcnq2 and PV was less common in layer V (Fig. 11*E–G*).

Kcnq2 and *Kcnq3*, along with *erg1*, were the genes most strongly expressed within the midbrain and hindbrain regions (Table 2, Fig. 12). The expression levels of Kcnq2 and the Kcnq3 in the brainstem were moderate, with many areas of overlap. Many of the brainstem nuclei expressing Kcnq2 and Kcnq3, such as medial vestibular nucleus, inferior olive, dorsal cochlear nucleus, pontine nucleus, inferior colliculus, substantia nigra, and red nucleus, also prominently expressed erg1 (Fig. 12). A few of the erg1-containing nuclei were also positive for erg3 (Table 2). Many of these nuclei contain heterogeneous populations of neurons. Therefore, to establish whether there is colocalization of EAG and Kcnq transcripts in brainstem neurons still requires an anal-

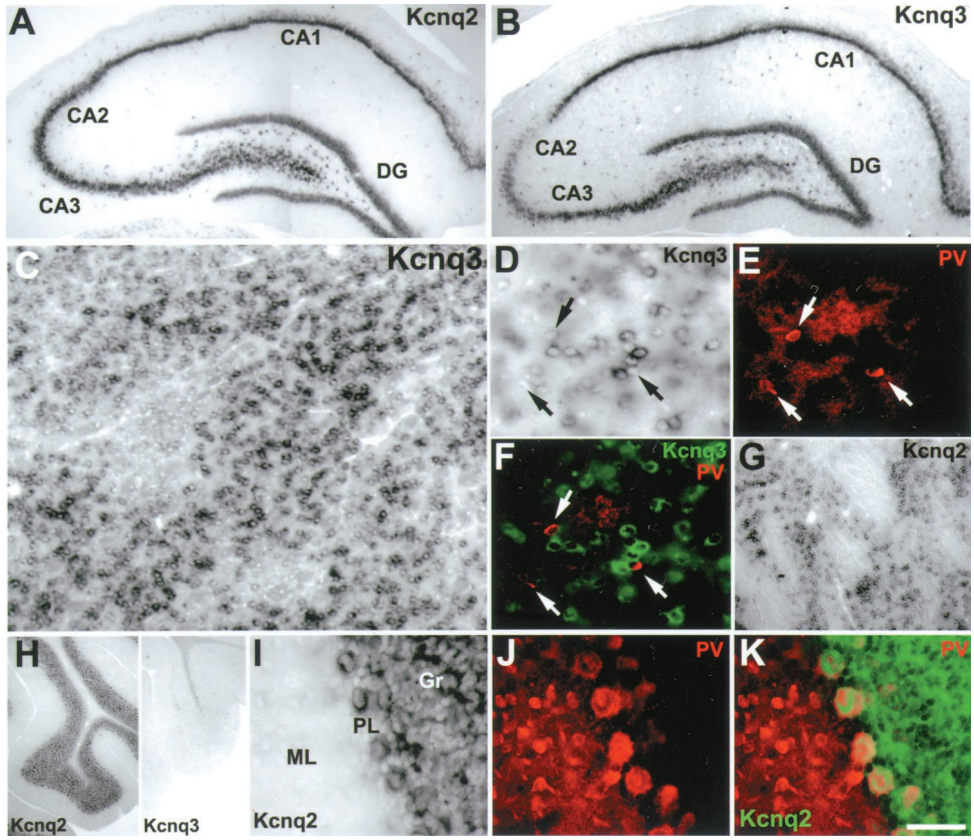

Figure 10. Kcnq2 and Kcnq3 mRNA transcripts overlap in the hippocampus and caudate/putamen, but not the cerebellum. *A–B*, Comparison of Kcnq2 and Kcnq3 transcripts in the hippocampus. *A*, Abundant Kcnq2 expression was detected in CA1–CA3 pyramidal cells and granule cells of the DG. *B*, Strong Kcnq3 expression was found in similar neurons but was weaker than Kcnq2 in CA2. *C–G*, Kcnq3 and Kcnq2 expression in the caudate/putamen (*CPu*). *C*, Low-magnification bright-field image showing strong Kcnq3 expression in the large majority of CPu neurons. *D–F*, Kcnq3 is not expressed in PV-immunoreactive neurons in the CPu. *D*, High-magnification bright-field image of Kcnq3-positive neurons in the CPu. *E*, Immunofluorescent detection of PV-containing neurons in same section as *D*. *F*, Overlay of *D* and *E* with Kcnq3 pseudocolored *green*. Note that no PV neurons were Kcnq3 positive (*arrows*). *G*, Kcnq2 is also located in the caudate/putamen. *H–K*, Kcnq2, but not Kcnq3, is expressed in the cerebellar cortex. *H*, Low-magnification image of Kcnq2 (*left*) and Kcnq3 (*right*) expression in the cerebellar cortex. *I–K*, Kcnq2 is located in the granule and Purkinje cell layer of the cerebellum. *I*, High-power bright-field image showing Kcnq2 expression in the cells of the Purkinje layer (*PL*) and granule layer (*Gr*) but not the molecular layer (*ML*). *J*, Same image as *I*, with immunodetection of PV-reactive Purkinje cells and interneurons of the molecular layer. *K*, Overlay of *I* and *J*, with Kcnq2 pseudocolored *green*. Scale bar (shown in *K*): *A*, *B*, 275 μm; *C*, 250 μm; *D–F*, 100 μm; *G*, 300 μm; *H*, 475 μm; *I–K*, 50 μm.

ysis of individual neuronal populations, but is likely to be extensive given the regional patterns observed in this study.

DISCUSSION

The M-current is a slow, non-inactivating K^+ current, believed to be one of the most important modulators of the subthreshold excitability of neurons and their responsiveness to synaptic inputs (Brown, 1988). The K^+ channels expressed in heterologous expression systems by subunits of the EAG family also have interesting properties (Table 3) and could have functional consequences similar to those of M-currents (Shi et al., 1997, 1998; Stansfeld et al., 1997; Meves et al., 1999; Saganich et al., 1999; Selyanko et al., 1999). Most EAG channels activate significantly at voltages close to physiological resting potentials and hence near or below the threshold for action potential generation (Table 3). Moreover, they have little or only incomplete inactivation. These low-threshold-activating channels could thus resemble M-channels in their ability to carry steady outward currents that can suppress the overall excitability of neurons and oppose action potential generation. Furthermore, the diversity in voltage-dependent and kinetic behavior, and perhaps distinct responses to neuromodulators, of the various channels of this group could provide neurons with divergent integrative properties and modulatory responses.

The presence of time-dependent relaxations of K^+ currents after hyperpolarization from depolarized (more than −40 mV) holding potentials has been interpreted typically as indicating the presence of M-channels. However, the closing of different types of EAG channels can produce similar relaxations, albeit with different kinetics. Moreover, muscarinic agonists also inhibit eag and erg channels (Stansfeld et al., 1996; Selyanko et al., 1999; Ludwig et al., 2000), demanding more detailed kinetic and pharmacological experiments to identify the channels mediating M-like currents in specific neurons. The distributions reported in this study will be an important aid in this process.

Roles for EAG potassium channels in the mammalian CNS remain to be found. However, the importance of these channels in the control of neuronal excitability in *Drosophila* (Wu at al., 1983; Ganetzky et al., 1999) and in human cardiac function (Curran et al., 1995; Sanguinetti, 1999) has been well established. The expression patterns shown here provide a framework to identify neurons in rodent brain where the roles of EAG family channels can be investigated.

Subunit composition of M-channels

It has been suggested that the channels mediating I_M in sympathetic neurons are heteromultimers of two members of the Kcnq family, Kcnq2 and Kcnq3 (Wang et al., 1998). When expressed alone, Kcnq2 channels produce small currents, whereas Kcnq3 proteins express negligible currents. It has been assumed that M-channels in the CNS have a subunit composition similar to that in sympathetic neurons, and therefore it was expected that cells expressing Kcnq3 subunits would also contain Kcnq2 proteins. Our results show that Kcnq2 and Kcnq3 transcripts indeed overlap in many neuronal populations, including neurons in which M-currents have been recorded [hippocampal pyramidal neurons (Madison and Nicoll, 1984); cortical layer V pyramidal cells (McCormick and Prince, 1986; Brown, 1988; Brown et al., 1990)]. However, to our surprise we also found that there are several neuronal populations that express one but not the other. For

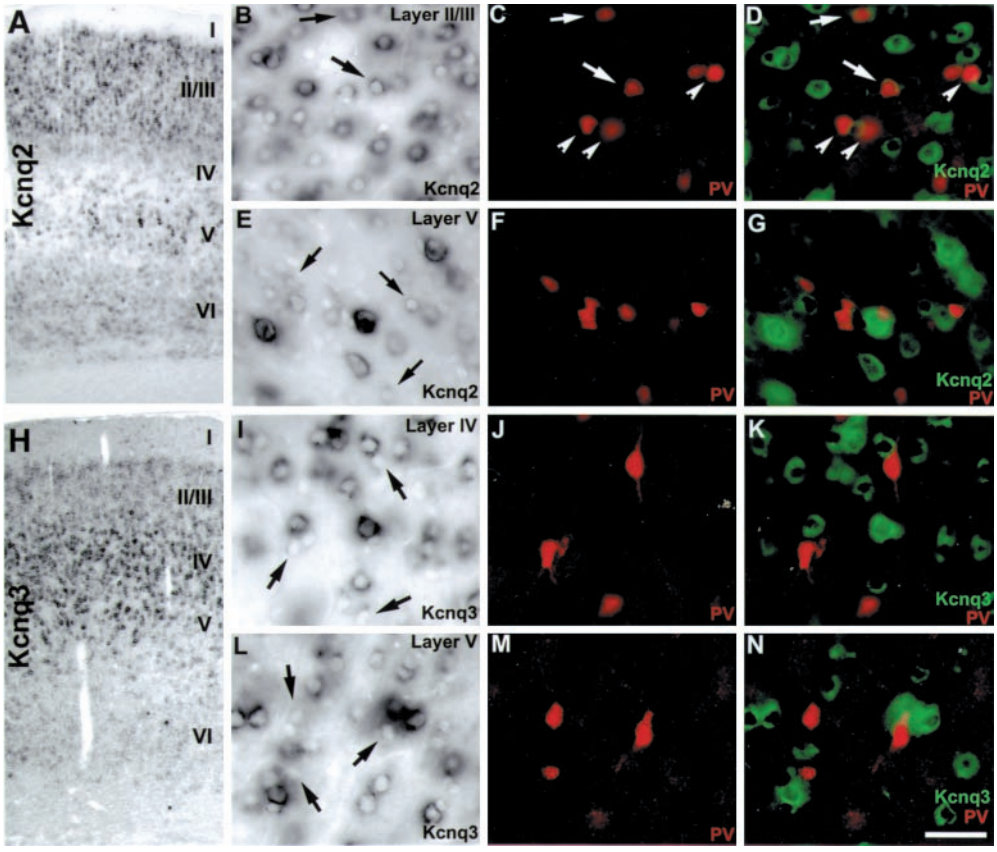

Figure 11. Differential distributions of Kcnq2 and Kcnq3 transcripts in rat cerebral cortex. *A*, Cross section of rat cerebral cortex showing strong Kcnq2-positive neurons in layers II/III and V, and little or no signal in layer IV. *B*, High-power bright-field image showing layer II/III Kcnq2-positive neurons. *C*, Same image as *B*, with immunodetection of PV-reactive interneurons. *D*, Overlay of *B–D* with Kcnq2 pseudocolored *green*. Note that some Kcnq2 transcripts colocalize with PV-positive interneurons (*B–D*, *arrows*), and some do not (*B–D*, *arrowheads*). *E*, High-power bright-field image showing strong Kcnq2 signal in a large layer V pyramidal neuron. *F*, Same image as *E*, with immunodetection of PV-reactive interneurons. *G*, Overlay of *E* and *F* with Kcnq2 pseudocolored *green*. Note that most Kcnq2 transcripts did not colocalize with PV-positive interneurons (*E*, *arrows*). *H*, ISH for Kcnq3 showing labeling of neurons in cortical layers II–VI, with highest levels found in layer IV. *I–N*, Kcnq3 expression is not found in PV-positive cortical interneurons in cortical layer IV (*I–K*) or V (*L–N*). *I*, High-power image of Kcnq3-labeled neurons in cortical layer IV. *J*, Immunofluorescent detection of PV in *I*. *K*, Overlay of *I* and *J* with Kcnq3 pseudocolored *green*. *L*, High-power image of Kcnq3-labeled neurons in cortical layer V. *M*, Immunofluorescent detection of PV in *L*. *N*, Overlay of *L* and *M* with Kcnq3 pseudocolored *green*. *Arrows* in *I* and *L* point to Kcnq3-negative cells that were immunoreactive for PV. Scale bar (shown in *N*): *A*, *H*, 200 μm; *B–G*, *I–N*, 50 μm.

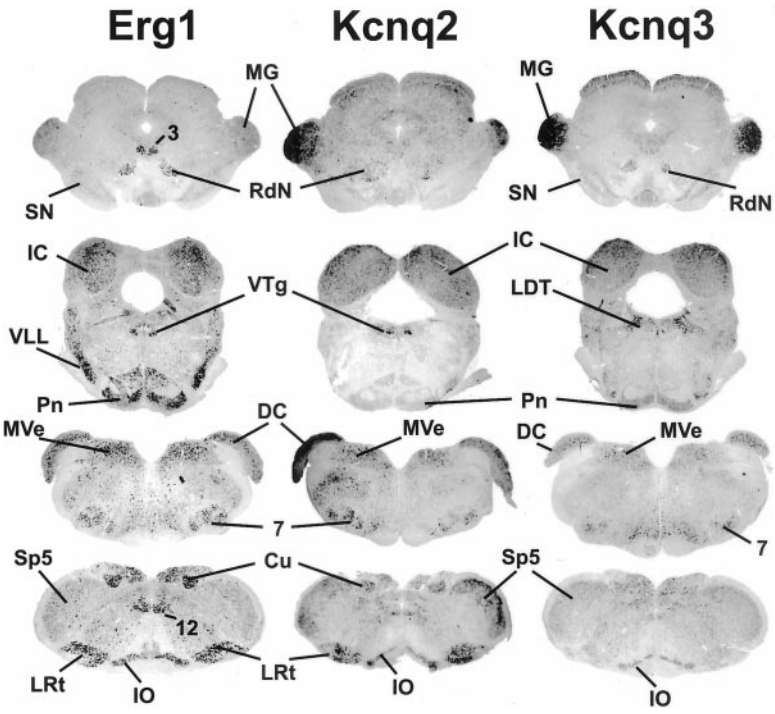

Figure 12. Erg1, Kcnq2, and Kcnq3 mRNA expression was often overlapping in the rat midbrain and hindbrain. *3*, Oculomotor nucleus; *7*, facial nucleus; *12,* hypoglossal nucleus; *Cu,* cuneate nucleus; *DC,* dorsal cochlear nucleus; *IC*, inferior colliculus; *IO*, inferior olive; *LDT*, laterodorsal tegmental nucleus; *LRt*, lateral reticular nucleus; *MG*, medial geniculate nucleus; *MVe*, medial vestibular nucleus; *Pn*, pontine nucleus; *RdN*, red nucleus; *SN*, substantia nigra; *Sp5*, spinal trigeminal nucleus; *VLL*, ventral nucleus lateral lemniscus; *VTg*, ventral tegmental nucleus.

example, Kcnq2 (but not Kcnq3) is prominently expressed in cerebellar granule and Purkinje cells (Figs. 1, 10, Table 2). On the other hand, Kcnq3 is strongly expressed in layer IV in the cortex, where Kcnq2 signals are weak (Figs. 1, 11, Table 2). These examples were particularly puzzling at the time when we completed these experiments, because the other two known members of the family, Kcnq1 and Kcnq4, either are not found in brain (Kcnq1) or are restricted to the brainstem auditory pathway

Table 3. Functional properties of EAG K^+ channels in heterologous expression systems

	Activation							Inactivation		Pharmacology (IC_{50})		
	V_{on} (mV)	$V_{1/2}$ (mV)	k (mV)	τ_{fast} (msec)	τ_{slow} (msec)	Cole–Moore shift	Deactivation τ_{deact} (msec)	τ_{inact} (msec)	τ_{recov} (msec)	TEA	4-AP	E-4031
Eag1	−60 to −50	−11.8 to −4.1	23.5	12 @ 40 mV[a]	210 @ 40 mV[a]	y	1–6	No inactivation		28	NB by 20 mM	NB
Eag2	−100	−35.5	29	14.6 @ 40 mV[a]	202 @ 40 mV[a]	y	Fast	No inactivation		19 @ 40 mV	NB by 20 mM	NB by 1 μM
Erg1	−60 to −50	−21	6 to 8	200 @ 0 mV		n	Seconds @ −70 mV	4.3 @ 30 mV	NA	Slows channel inactivation	NA	K_D 99 nM
Erg2	−40	−3.5	8.3	111 @ 0 mV	500 @ 0 mV	n	Seconds @ −70 mV	4.7 @ 30 mV	NA	NA	NA	K_D 116 nM
Erg3	−80 to −70	−44	7.2	25 @ 0 mV		n	~100 @ −70 mV	8 @ 30 mV	NA	NA	NA	K_D 193 nM
Elk1	−40	9.3	13.1	676 @ 0 mV		n	111 @ −50 mV	No inactivation		NB by 10 mM	NB by 10 mM	NB by 10 μM
Elk2	−80 to −70	−6.4 to −24.4	20.1 to 28.3	7.7 @ 30 mV	70.0 @ 30 mV	n	τ_{fast} = 93.7 τ_{slow} = 622 @ −50 mV	10.2 @ 30 mV	6.7 @ −50 mV	Slows channel inactivation	NA	NB by 10 μM
Elk3	−90	−59.1	10.8	38 @ 0 mV	360 @ 0 mV	n	201 @ −80 mV	No inactivation		NB by 100 mM	NB by 10 mM	NB by 10 μM

Data were obtained from Ludwig et al. (1994), Robertson et al. (1996), Terlau et al. (1996), Shi et al. (1997, 1998), Bijlenga et al. (1998), Engeland et al. (1998), Frings et al. (1998), Saganich et al. (1999), Schonherr et al. (1999), and Trudeau et al. (1999).

y, Yes; n, no; NA, not available; NB, not blocked; V_{on}, "activation" voltage; time constants at room temperature.

[a] Holding potential = −90 mV.

(Kcnq4) (Coetzee et al., 1999; Kubisch et al., 1999; Kharkovets et al., 2000). While our experiments were in progress, a new Kcnq subunit, Kcnq5, was identified (Lerche et al., 2000; Schroeder et al., 2000). This subunit has also been shown to coassemble with Kcnq3 proteins and produce M-channels *in vitro*, suggesting that it contributes to the formation of M-channels in brain. Moreover, Kcnq5 mRNAs are strongly expressed in the neocortex (Schroeder et al., 2000). It is thus possible that Kcnq5 forms heteromultimeric M-channels with Kcnq3 in cortical layer IV neurons. More puzzling at present is the situation in the cerebellar cortex, where Kcnq5 is expressed very weakly (Schroeder et al., 2000).

Heteromultimeric EAG-family channels

Recent evidence shows that different members of one of the EAG subfamilies (erg) can heteromultimerize to form channels with novel electrophysiological properties when coexpressed in Chinese hamster ovary cells (Wimmers et al., 2001). Furthermore, erg subunits do not seem to coassemble with eag or elk proteins (Wimmers et al., 2001). Further investigation of the ability of EAG family members to heteromultimerize within and between different subfamilies is still necessary to uncover the "rules" that govern EAG channel assembly; however, it is quite possible that a situation similar to that observed in the Kv family of K^+ channels will emerge in the EAG family. In the Kv family, members of the same subfamily, but not of different subfamilies, can form heteromeric channels in heterologous expression systems, and heteromeric complexes have been shown to exist in brain tissue (Coetzee et al., 1999). Our data show overlap of multiple members of the same EAG subfamily in the same neuronal population in which they may form heteromeric channels. Moreover, different combinations of subunits of a given EAG subfamily are found in different neuron types. For example, both erg1 and erg3 transcripts are expressed in cerebellar Purkinje cells and the neurons of the reticular thalamus, but erg1 is found alone in the basket cells of the hippocampus (Figs. 1, 5, 6, Table 2). Therefore, as in the case of Kv channels, the subunit composition (and perhaps the functional properties) of EAG channels containing a particular subunit, could vary between different neurons (Weiser et al., 1994; Coetzee et al., 1999).

Multiple channels may contribute to the subthreshold K^+ current in many CNS neurons

This study showed that many neurons contain transcripts for multiple subthreshold EAG and/or Kcnq channels. For example, on the basis of the observation that most layer V pyramidal neurons contained Kcnq2, Kcnq3, eag1, erg1, and erg3, it is very likely that all of these transcripts are coexpressed in many of these neurons. Pyramidal cells in the hippocampus also coexpressed multiple EAG and Kcnq mRNAs, as did neurons in several other brain areas (see Table 2, and the appropriate sections in Results). In contrast, other neurons, such as inhibitory interneurons in the hippocampus, had only a single member (erg1), as judged by colocalization with inhibitory cell markers.

Although it still remains to be shown that the protein products are expressed and localized in somatodendritic membrane, this overlap of multiple EAG and Kcnq transcripts suggests the possibility that the voltage-dependent subthreshold K^+ current of many neurons may include the contribution of different components, produced by channels with different properties, including distinct responses to neuromodulators. The situation in many CNS neurons may resemble that recently described for the native M-like currents in neuroblastoma NG108–15 cells. The I_M of these cells was shown to include a Kcnq2–Kcnq-3-mediated component resembling the M-current in sympathetic neurons, and a slower component probably mediated by channels containing erg proteins (Meves et al., 1999; Selyanko et al., 1999).

Of additional interest was the observation that cortical inhibitory interneurons seem to express few members of the EAG or Kcnq family in comparison to local and projecting excitatory neurons. The only clear exception was erg1, which seemed to be prominent in populations of inhibitory interneurons in several brain areas, including neocortex and hippocampus. Differences in

the expression and properties of M-channels and other subthreshold currents in inhibitory interneurons compared with excitatory neurons could result in markedly different susceptibilities to subthreshold modulation of excitability.

The complexity of subthreshold K^+ currents in neurons is further increased by currents from inward rectifiers (particularly those displaying weak rectification) and "leak" K^+ channels composed of proteins of the recently discovered tandem or two-pore K^+ channel family (Goldstein et al., 1998). The window current of subthreshold-activating A-type K^+ currents and the contributions from Kv1 channels showing sufficient activation in the subthreshold voltage range (such as those mediating the slowly and incompletely inactivating D current), and under some conditions calcium-activating K^+ currents, can also contribute to this complexity. How these different channels impact neuronal excitability remains to be explored. This diversity may be partially associated with differential subcellular localization of the channels (Cooper et al., 2000). This is an issue of great importance and will require the development of specific antibodies to determine the localization of protein products. For example, localization of multiple subthreshold operating channels with diverse kinetics and voltage responses in compartments receiving synaptic inputs provides a substrate for tuning cells to differentially filter synaptic inputs. An analogous role has already been described for A-currents on AMPA versus NMDA responses (Schoppa et al., 1999). Distinct subthreshold-operating channels may also respond differently to neuromodulators, allowing specific temporal and spatial control of the membrane impedance and the resting potential.

REFERENCES

Abbott GW, Sesti F, Splawski I, Buck ME, Lehmann MH, Timothy KW, Keating MT, Goldstein SA (1999) MiRP1 forms IKr potassium channels with HERG and is associated with cardiac arrhythmia. Cell 97:175–187.

Baxter DA, Byrne JH (1991) Ionic conductance mechanisms contributing to the electrophysiological properties of neurons. Curr Opin Neurobiol 1:105–112.

Bijlenga P, Occhiodoro T, Liu JH, Bader CR, Bernheim L, Fischer-Lougheed J (1998) An ether-a-go-go K+ current, Ih-eag, contributes to the hyperpolarization of human fusion-competent myoblasts. J Physiol (Lond) 512:317–323.

Brown DA (1988) M channels. In: Ion channels (Narahashi ET, ed), pp 55–94. New York: Plenum.

Brown DA, Adams PR (1980) Muscarinic suppression of a novel voltage-sensitive K+ current in a vertebrate neurone. Nature 283:673–676.

Brown DA, Gahwiler BH, Griffith WH, Halliwell JV (1990) Membrane currents in hippocampal neurons. Prog Brain Res 83:141–160.

Chow A, Erisir A, Farb C, Nadal MS, Ozaita A, Lau D, Welker E, Rudy B (1999) K(+) channel expression distinguishes subpopulations of parvalbumin- and somatostatin-containing neocortical interneurons. J Neurosci 19:9332–9345.

Coetzee W, Amarillo Y, Chiu J, Chow A, Lau D, McCormack T, Moreno H, Nadal MS, Ozaita A, Pountney D, Saganich M, Vega-Saenz de Miera E, Rudy B (1999) Molecular diversity of K^+ channels. Ann NY Acad Sci 868:233–285.

Connor JA, Stevens CF (1971) Prediction of repetitive firing behaviour from voltage clamp data on an isolated neurone soma. J Physiol (Lond) 213:31–53.

Cooper EC, Aldape DK, Abosch A, Barbaro NM, Berger MS, Peacock WS, Jan NY, Jan LY (2000) Colocalization and coassembly of two human brain M-type potassium channel subunits that are mutated in epilepsy. Proc Natl Acad Sci USA 97:4914–4919.

Crespo C, Alonso JR, Brinon JG, Weruaga E, Porteros A, Arevalo R, Aijon J (1997) Calcium-binding proteins in the periglomerular region of typical and atypical olfactory glomeruli. Brain Res 745:293–302.

Curran ME, Splawski I, Timothy KW, Vincent GM, Green ED, Keating MT (1995) A molecular basis for cardiac arrhythmia: HERG mutations cause long QT syndrome. Cell 80:795–803.

Egger V, Sackmann B (2001) Symmetry and asymmetry of excitatory spiny stellate and star pyramid neurons in layer 4 of rat barrel cortex including their axons. Barrels XIII Abstr. Somatosens Mot Res, in press.

Engeland B, Neu A, Ludwig J, Roeper J, Pongs O (1998) Cloning and functional expression of rat ether-a-go-go-like K+ channel genes. J Physiol (Lond) 513:647–654.

Freund TF, Buzsaki G (1996) Interneurons of the hippocampus. Hippocampus 6:347–470.

Frings S, Brull N, Dzeja C, Angele A, Hagen V, Kaupp UB, Baumann A (1998) Characterization of ether-a-go-go channels present in photoreceptors reveals similarity to IKx, a K+ current in rod inner segments. J Gen Physiol 111:583–599.

Ganetzky B, Robertson AG, Wilson FG, Trudeau MC, Titus SA (1999) The Eag Family of K^+ channels in *Drosophila* and mammals. Ann NY Acad Sci 868:356–369.

Goldstein SA, Wang KW, Ilan N, Pausch MH (1998) Sequence and function of the two P domain potassium channels: implications of an emerging superfamily. J Mol Med 76:13–20.

Halliwell JV (1986) M-current in human neocortical neurones. Neurosci Lett 67:1–6.

Heimer L, Zahm D, Alheid G (1995) Basal ganglia. In: The rat nervous system (Paxinos G, ed), pp 579–628. San Diego: Academic.

Hernandez-Pineda R, Chow A, Amarillo Y, Moreno H, Saganich M, Vega-Saenz de Miera EC, Hernandez-Cruz A, Rudy B (1999) Kv3.1–Kv3.2 channels underlie a high-voltage-activating component of the delayed rectifier K+ current in projecting neurons from the globus pallidus. J Neurophysiol 82:1512–1528.

Hille B (1992) Ionic channels of excitable membranes. Sunderland, MA: Sinauer.

Hoffman DA, Magee JC, Colbert CM, Johnston D (1997) K+ channel regulation of signal propagation in dendrites of hippocampal pyramidal neurons. Nature 387:869–875.

Hontanilla, B, Parent, A, de las Heras, S, Gimenez-Amaya JM (1998) Distribution of calbindin D-28k and parvalbumin neurons and fibers in the rat basal ganglia. Brain Res Bull 47:107–116.

Johnston D, Hoffman DA, Colbert CM, Magee JC (1999) Regulation of back-propagating action potentials in hippocampal neurons. Curr Opin Neurobiol 9:288–292.

Jones EG (1985) The thalamus. New York: Plenum.

Kawaguchi Y, Kubota Y (1997) GABAergic cell subtypes and their synaptic connections in rat frontal cortex. Cereb Cortex 7:476–486.

Kharkovets T, Hardelin JP, Safieddine S, Schweizer M, El-Amraoui A, Petit C, Jentsch TJ (2000) KCNQ4, a K+ channel mutated in a form of dominant deafness, is expressed in the inner ear and the central auditory pathway. Proc Natl Acad Sci USA 97:4333–4338.

Kita H, Kosaka T, Heizmann CW (1990) Parvalbumin-immunoreactive neurons in the rat neostriatum: a light and electron microscopic study. Brain Res 536:1–15.

Kubisch C, Schroeder BC, Friedrich T, Lutjohann B, El-Amraoui A, Marlin S, Petit C, Jentsch TJ (1999) KCNQ4, a novel potassium channel expressed in sensory outer hair cells, is mutated in dominant deafness. Cell 96:437–446.

Lerche C, Scherer CR, Seebohm G, Derst C, Wei AD, Busch AE, Steinmeyer K (2000) Molecular cloning and functional expression of KCNQ5, a potassium channel subunit that may contribute to neuronal M-current diversity. J Biol Chem 275:22395–22400.

Ludwig J, Terlau H, Wunder F, Bruggemann A, Pardo LA, Marquardt A, Stuhmer W, Pongs O (1994) Functional expression of a rat homologue of the voltage gated ether-a-go-go potassium channel reveals differences in selectivity and activation kinetics between the *Drosophila* channel and its mammalian counterpart. EMBO J 13:4451–4458.

Ludwig J, Weseloh R, Karschin C, Liu Q, Netzer R, Engeland B, Stansfeld C, Pongs O (2000) Cloning and functional expression of rat eag2, a new member of the ether-a-go-go family of potassium channels and comparison of its distribution with that of eag1. Mol Cell Neurosci 16:59–70.

Madison DV, Nicoll RA (1984) Control of the repetitive discharge of rat CA 1 pyramidal neurones in vitro. J Physiol (Lond) 354:319–331.

McCormack K, Lin JW, Iverson LE, Rudy B (1990) Shaker K+ channel subunits from heteromultimeric channels with novel functional properties. Biochem Biophys Res Commun 171:1361–1371.

McCormick DA (1992) Neurotransmitter actions in the thalamus and cerebral cortex and their role in neuromodulation of thalamocortical activity. Prog Neurobiol 39:337–388.

McCormick DA, Prince DA (1986) Mechanisms of action of acetylcholine in the guinea-pig cerebral cortex in vitro. J Physiol (Lond) 375:169–194.

McCormick DA, Williamson A (1989) Convergence and divergence of neurotransmitter action in human cerebral cortex. Proc Natl Acad Sci USA 86:8098–8102.

Meves H, Schwarz JR, Wulfsen I (1999) Separation of M-like current and ERG current in NG108–15 cells. Br J Pharmacol 127:1213–1223.

Miyake A, Mochizuki S, Yokoi H, Kohda M, Furuichi K (1999) New ether-a-go-go K(+) channel family members localized in human telencephalon. J Biol Chem 274:25018–25025.

Robertson GA, Warmke JM, Ganetzky B (1996) Potassium currents expressed from *Drosophila* and mouse eag cDNAs in *Xenopus* oocytes. Neuropharmacology 35:841–850.

Rudy B (1988) Diversity and ubiquity of K channels. Neuroscience 25:729–749.
Saganich MJ, Vega-Saenz de Miera E, Nadal MS, Baker H, Coetzee WA, Rudy B (1999) Cloning of components of a novel subthreshold-activating K(+) channel with a unique pattern of expression in the cerebral cortex. J Neurosci 19:10789–10802.
Sanguinetti MC (1999) Dysfunction of delayed rectifier potassium channels in an inherited cardiac arrythmia. Ann NY Acad Sci 868:406–411.
Sanguinetti MC, Jiang C, Curran ME, Keating MT (1995) A mechanistic link between an inherited and an acquired cardiac arrhythmia: HERG encodes the IKr potassium channel. Cell 81:299–307.
Schonherr R, Hehl S, Terlau H, Baumann A, Heinemann SH (1999) Individual subunits contribute independently to slow gating of bovine EAG potassium channels. J Biol Chem 274:5362–5369.
Schoppa NE, Westbrook GL (1999) Regulation of synaptic timing in the olfactory bulb by an A-type potassium current. Nat Neurosci 2:1106–1113.
Schroeder BC, Kubisch C, Stein V, Jentsch TJ (1998) Moderate loss of function of cyclic-AMP-modulated KCNQ2/KCNQ3 K+ channels causes epilepsy. Nature 396:687–690.
Schroeder BC, Hechenberger M, Weinreich F, Kubisch C, Jentsch TJ (2000) KCNQ5, a novel potassium channel broadly expressed in brain, mediates M-type currents. J Biol Chem 275:24089–24095.
Selyanko AA, Hadley JK, Wood IC, Abogadie FC, Delmas P, Buckley NJ, London B, Brown DA (1999) Two types of K(+) channel subunit, Erg1 and KCNQ2/3, contribute to the M-like current in a mammalian neuronal cell. J Neurosci 19:7742–7756.
Sheng M, Liao YJ, Jan YN, Jan LY (1993) Presynaptic A-current based on heteromultimeric K+ channels detected in vivo. Nature 365:72–75.
Shi W, Wymore RS, Wang HS, Pan Z, Cohen IS, McKinnon D, Dixon JE (1997) Identification of two nervous system-specific members of the erg potassium channel gene family. J Neurosci 17:9423–9432.
Shi W, Wang HS, Pan Z, Wymore RS, Cohen IS, McKinnon D, Dixon JE (1998) Cloning of a mammalian elk potassium channel gene and EAG mRNA distribution in rat sympathetic ganglia. J Physiol (Lond) 511:675–682.
Stansfeld CE, Roper J, Ludwig J, Weseloh RM, Marsh SJ, Brown DA, Pongs O (1996) Elevation of intracellular calcium by muscarinic receptor activation induces a block of voltage-activated rat ether-a-go-go channels in a stably transfected cell line. Proc Natl Acad Sci USA 93:9910–9914.
Stansfeld C, Ludwig J, Roeper J, Weseloh R, Brown D, Pongs O (1997) A physiological role for ether-a-go-go K+ channels? Trends Neurosci 20:13–14.
Terlau H, Ludwig J, Steffan R, Pongs O, Stuhmer W, Heinemann SH (1996) Extracellular Mg2+ regulates activation of rat eag potassium channel. Pflügers Arch 432:301–312.
Tinel N, Lauritzen I, Chouabe C, Lazdunski M, Borsotto M (1998) The KCNQ2 potassium channel: splice variants, functional and developmental expression. Brain localization and comparison with KCNQ3. FEBS Lett 438:171–176.
Trudeau MC, Warmke JW, Ganetzky B, Robertson GA (1995) HERG, a human inward rectifier in the voltage-gated potassium channel family. Science 269:92–95.
Trudeau MC, Titus SA, Branchaw JL, Ganetzky B, Robertson GA (1999) Functional analysis of a mouse brain Elk-type K+ channel. J Neurosci 19:2906–2918.
Wang H, Kunkel DD, Martin TM, Schwartzkroin PA, Tempel BL (1993) Heteromultimeric K+ channels in terminal and juxtaparanodal regions of neurons. Nature 365:75–79.
Wang HS, Pan Z, Shi W, Brown BS, Wymore RS, Cohen IS, Dixon JE, McKinnon D (1998) KCNQ2 and KCNQ3 potassium channel subunits: molecular correlates of the M-channel. Science 282:1890–1893.
Warmke JW, Ganetzky B (1994) A family of potassium channel genes related to eag in *Drosophila* and mammals. Proc Natl Acad Sci USA 91:3438–3442.
Weiser M, Vega-Saenz de Miera E, Kentros C, Moreno H, Franzen L, Hillman D, Baker H, Rudy B (1994) Differential expression of Shaw-related K+ channels in the rat central nervous system. J Neurosci 14:949–972.
Wimmers S, Wulfsen I, Bauer CK, Schwarz JR (2001) Erg1, erg2 and erg3 K channel subunits are able to form heteromultimers. Pflügers Arch 441:450–455.
Wu CF, Ganetzky B, Haugland FN, Liu AX (1983) Potassium currents in *Drosophila*: different components affected by mutations of two genes. Science 220:1076–1078.
Yamada WM, Koch C, Adams PR (1989) Methods in neuronal modeling (Koch C, Segev I, eds), pp 97–133. Cambridge, MA: Bradford.